

This publication is a Validated Methods, Reference Methods and Measurements by the Joint Research Centre (JRC), the European Commission's science and knowledge service. It aims to provide evidence-based scientific support to the European policy making process. The contents of this publication do not necessarily reflect the position or opinion of the European Commission. Neither the European Commission nor any person acting on behalf of the Commission is responsible for the use that might be made of this publication. For information on the methodology and quality underlying the data used in this publication for which the source is neither Eurostat nor other Commission services, users should contact the referenced source. The designations employed and the presentation of material on the maps do not imply the expression of any opinion whatsoever on the part of the European Union concerning the legal status of any country, territory, city or area or of its authorities, or concerning the delimitation of its frontiers or boundaries.

Contact information

Name: Thomas Malkow

Address: European Commission, Joint Research Centre, Westerduinweg 3, 1755 LE Petten, The Netherlands

Email: Thomas.Malkow@ec.europa.eu

Tel.: +31 224 56 56 56

EU Science Hub

<https://joint-research-centre.ec.europa.eu>

JRC129387

Print ISBN 978-92-76-61557-6 doi:10.2760/7940 KJ-03-22-290-EN-C

PDF ISBN 978-92-76-61556-9 doi:10.2760/31803 KJ-03-22-290-EN-N

Luxembourg: Publications Office of the European Union, 2023

© European Union, 2023



The reuse policy of the European Commission documents is implemented by the Commission Decision 2011/833/EU of 12 December 2011 on the reuse of Commission documents (OJ L 330, 14.12.2011, p. 39). Unless otherwise noted, the reuse of this document is authorised under the Creative Commons Attribution 4.0 International (CC BY 4.0) licence (<https://creativecommons.org/licenses/by/4.0/>). This means that reuse is allowed provided appropriate credit is given and any changes are indicated.

For any use or reproduction of photos or other material that is not owned by the European Union, permission must be sought directly from the copyright holders. The European Union does not own the copyright in relation to the following elements:

- page 3, CEA logo, source: <https://www.cea.fr>,
- page 3, DTU logo, source: <https://www.dtu.dk>,
- page 3, DLR logo, source: <https://www.dlr.de>,
- page 3, EIfER logo, source: <https://www.eifer.kit.edu>,
- page 3, Kiwa logo, source: <https://www.kiwa.com>,
- page 3, PIPC logo, source: <https://pipc.org.pl>,
- page 3, SINTEF logo, source: <https://www.sintef.no>,
- page 3, Shell logo, source: <https://www.shell.com>,
- page 3, TNO logo, source: <https://www.tno.nl> and
- page 3, Univ Genova logo, source: <https://unige.it>.

How to cite this report: Malkow, T., Pilenga, A.; *EU harmonised testing protocols for high-temperature steam electrolysis*; Publications Office of the European Union, Luxembourg, 2023; doi:10.2760/31803; JRC129387.

Contents

Abstract.....	1
Foreword.....	2
Acknowledgements.....	3
1 Introduction.....	4
2 Objective and scope of this document.....	6
3 Overview of high-temperature steam electrolysis technologies.....	8
3.1 High-temperature steam electrolysis electrode reactions.....	8
3.2 Materials, configurations and technology readiness levels.....	9
3.3 Operation modes of HTE stacks.....	9
4 Terminology.....	11
4.1 Terms and definitions.....	11
4.2 Abbreviations and acronyms used.....	13
4.3 Symbols used.....	13
5 Description of test items.....	14
5.1 HTE stack.....	14
5.2 HTSEL system.....	15
6 Testing protocols.....	17
6.1 General.....	17
6.2 Test conditions.....	17
6.3 Reference test conditions.....	18
6.4 Measurement techniques.....	18
6.5 Test plan.....	18
6.6 Performance tests.....	19
6.6.1 Input electric power.....	19
6.6.2 Input thermal power.....	20
6.6.3 Input power of compression.....	20
6.6.4 Start-up time and energy.....	20
6.6.5 Response time and ramp energy.....	20
6.6.6 Shut-down time and energy.....	20
6.6.7 Switch-over time.....	20
6.6.8 Hydrogen output rate and quality.....	20
6.6.9 Oxygen output rate and quality.....	21
6.6.10 Polarisation curve measurements.....	21
6.6.11 Electrochemical imittance spectroscopy measurements.....	21
6.6.12 Specific energy consumption.....	22
6.6.13 Efficiency.....	22
6.7 Operation profiles.....	23
6.7.1 General.....	23
6.7.2 Graphical representation.....	23

6.8 Durability tests.....	26
6.8.1 General.....	26
6.8.2 Constant stack operation.....	26
6.8.3 Variable stack operation.....	26
6.8.4 KPI estimation.....	26
7 Presentation of test results	31
8 Conclusions with final remarks.....	35
References.....	36
List of Abbreviations and Acronyms	40
List of Symbols.....	43
List of Figures.....	47
List of Tables.....	48
Annexes.....	49
Annex A Test safety.....	49
Annex B Tabulated data of operation profiles.....	50
B.1 Reactivity operation profile.....	50
B.2 Flexibility operation profiles.....	53
Annex C Test report.....	62
C.1 General.....	62
C.2 Title page.....	62
C.3 Summary report.....	62

Abstract

The objective of this document is to present testing protocols for establishing the performance and durability of high-temperature electrolyser (HTE) stacks and high-temperature steam electrolysis (HTSEL) systems for the generation of bulk amounts of hydrogen by the electrolysis of steam (water vapour) using electricity mostly from variable renewable energy sources (RESs). In addition, stacks and systems may utilise heat from energy conversion, natural resources (geothermal and solar) and industrial processes.

By applying these testing protocols, it will be generally possible to characterise and evaluate the performance and durability of different stacks and systems aiming at an adequate comparison of two HTSEL technologies namely solid oxide steam electrolysis (SOEL) and proton-conducting ceramic steam electrolysis (PCCEL).

The test methods contained herein are based on standards of the International Organization for Standardization (ISO) and the International Electrotechnical Commission (IEC). In addition, we consider testing procedures previously developed by European Union (EU) funded research projects as well as those published as part of the EU electrolysis harmonisation activities. Presented operation profiles serve as examples and may be complemented by more appropriate profiles, for example, to reflect realistic RES power profiles for on-demand HTE stack operation.

These testing protocols are intended to be used by the research community and industry alike, for example, to evaluate research and development (R&D) progress, set research and innovation (R&I) priorities including cost targets, development milestones and technological benchmarks as well as making informed decisions regarding technology selection in power-to-hydrogen (P2H2) and hydrogen-to-industry (H2I) applications.

Foreword

This report was carried out under the framework contract between the Directorate-General JRC of the European Commission (EC) and the Fuel Cells and Hydrogen second Joint Undertaking (FCH2JU), the predecessor to the Clean Hydrogen Joint Undertaking (Clean H₂ JU) ⁽¹⁾. The JRC contractual activities are summarised in the strategic research and innovation agenda 2021-2027 of the Clean Hydrogen Partnership for Europe (SRIA) ⁽²⁾. This report constitutes the deliverable B.3 of the Rolling Plan 2022, contained in the Clean H₂ JU work programme 2022 ⁽³⁾. It is the result of a collaborative effort between European partners from research and technology organisations in industry and academia participating to EU funded R&D projects ⁽⁴⁾ in P2H2 and H2I applications involving HTE for demonstration and eventually, industrial deployment.



⁽¹⁾ According to Article 3(1)(c) of Council Regulation (EU) No 2021/2085 of 19/11/2021 (EU OJ L 427, 30.11.2021, p. 17), the Clean H₂ JU succeeds the FCH2JU as of 30 November 2021.

⁽²⁾ see online at https://www.clean-hydrogen.europa.eu/about-us/key-documents/strategic-research-and-innovation-agenda_en on p. 103

⁽³⁾ see online at https://www.clean-hydrogen.europa.eu/about-us/key-documents/annual-work-programmes_en on p. 209

⁽⁴⁾ For a list of projects, see online at https://www.clean-hydrogen.europa.eu/projects-repository_en. More comprehensive information can be searched at the Community Research and Development Information Service (CORDIS) under <https://cordis.europa.eu>.

Acknowledgements

We would like to express our sincere gratitude to all participants and their respective organisations (see below) for useful and valuable contributions in developing this report. In addition, we appreciate the opportunity to rely on existent testing protocols and test procedures developed in the EU funded research projects MultiPLHY ⁽⁵⁾, REFLEX ⁽⁶⁾, GAMER ⁽⁷⁾ and SOCTESQA ⁽⁸⁾ as well as on standards drafted by ISO and IEC. We also thank the Clean H₂ JU for financial support.

Authors: Malkow, T., Pilenga, A.

Note: Contributors are listed in alphabetical order according to the name of their participating organisation.

	Organisation	Contributor(s)
	Commissariat à l'énergie atomique et aux énergies alternatives (CEA)	Julie Mougin
	Danmarks Tekniske Universitet (DTU)	Xiufu Sun
	Deutsches Zentrum für Luft- und Raumfahrt e. V. (DLR)	Michael Lang Matthias Riegraf
	Europäisches Institut für Energieforschung (ElFER)	Elisa Effori
	Kiwa NV	Stephen John McPhail
	Polska Izba Przemysłu Chemicznego (PIPC)	Michalina Ewa Michniewicz Mateusz Potocki
	Stiftelsen for industriell og teknisk forskning (SINTEF)	Marie-Laure Fontaine
	Shell Global Solutions International BV	Arian Nijmeijer Peter Veenstra
	Nederlandse Organisatie voor Toegepast Natuurwetenschappelijk Onderzoek (TNO)	Frans F P van Berkel Eduardo Da Rosa Silva Michiel Langerman Maciej K Stodolny
	Università di Genova	Fiammetta Rita Bianchi Barbara Bosio

⁽⁵⁾ Multimegawatt high-temperature electrolyser to generate green hydrogen for production of high-quality biofuels coordinated by CEA with Sunfire GmbH, Neste Oyj, Neste Netherlands BV and Neste Engineering Solutions BV as partners

⁽⁶⁾ Reversible solid oxide Electrolyzer and Fuel cell for optimized Local Energy miX coordinated by CEA with DTU, Teknologian tutkimuskeskus VTT Oy (VTT), Green Power Technologies, S.L., Elcogen AS, Sylfen, Engie SA, Parco Scientifico Tecnologico per l'Ambiente and Universidad de Sevilla as partners

⁽⁷⁾ Game changer in high temperature steam electrolyzers with novel tubular cells and stacks geometry for pressurized hydrogen production coordinated by SINTEF AS with CoorsTek Membrane Sciences AS (CMS), Consejo Superior de Investigaciones Científicas (CSIC), Carbon Recycling International EHF (CRI), Universitetet i Oslo (UiO), MC2 Ingeniería Y Sistemas S.L. and Shell Global Solutions International BV as partners

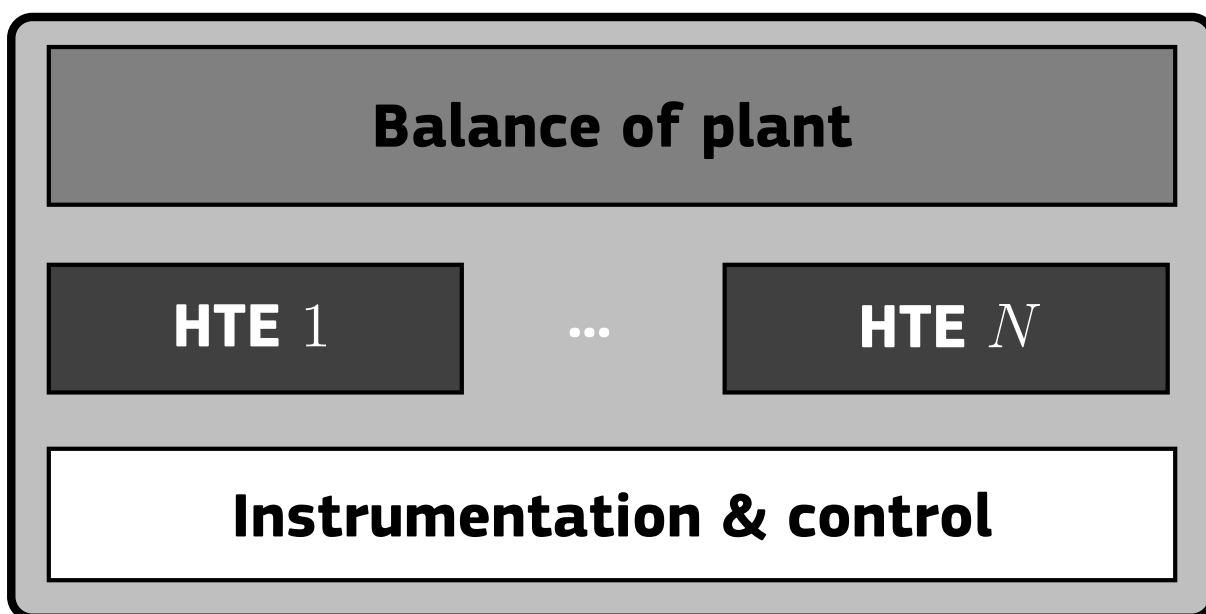
⁽⁸⁾ Solid Oxide Cell and Stack Testing, Safety and Quality Assurance coordinated by DLR with CEA, DTU, Agenzia Nazionale per le Nuove tecnologie, l'Energia e lo Sviluppo economico sostenibile (ENEA), JRC and ElFER as partners

1 Introduction

HTE stacks and HTSEL systems (Figure 1.1) increasingly play an important role for the generation of bulk amounts of hydrogen (H_2) by HTSEL in P2H2 applications and H2I processes. They use electricity particularly from variable RESs and heat (thermal energy) from energy conversion, natural resources (geothermal and solar energy) and industrial processes making them, in principle, more energy efficient than their more mature counterparts using commercially readily available low-temperature water electrolysis (LTWE) technologies (section 3.3): alkaline water electrolysis (AEL) in alkaline water electrolyser (AWE) and proton exchange polymer membrane water electrolysis (PEMEL) in proton exchange polymer membrane water electrolyser (PEMWE) (Chatenet *et al.*, 2022, Shih *et al.*, 2022, Ebbesen *et al.*, 2014).

Solid oxide cell (SOC) technologies comprise both solid oxide electrolysis cells (SOECs) in solid oxide electrolyser (SOE) including reversible solid oxide electrolysis cell (rSOC) in reversible solid oxide electrolyser (rSOE) and proton-conducting ceramic electrolysis cells (PCECs) in proton-conducting ceramic electrolyser (PCE) including reversible proton-conducting ceramic electrolysis cell (rPCC) in reversible proton-conducting ceramic electrolyser (rPCE).

Figure 1.1: Schematic of a HTSEL system comprising one or more HTE stacks (HTE 1 to N), common balance of plant (BoP) and instrumentation & control devices including safety sensors and software.



Source: JRC, 2022.

Commonly, the manufacturer specifies which BoP components form part of the system. Besides common hardware (piping, valves, actuators, sensors, wiring/cabling, etc.), BoP usually consists of

- **power supply** such as an alternating current-to-direct current (AC/DC) converter (rectifier) when grid-connected, or direct current-to-direct current (DC/DC) converter(s) when directly coupled (off-grid) to one or another RES, for example, photovoltaic (PV) arrays and/or wind turbines,
- **steam generator** for feeding steam to the HTE stack(s) or **conditioning unit** for supplied steam and
- **hydrogen processing unit** including gas purification, cooler(s), dryer(s) and steam-trap.

The immediate use of the generated hydrogen may require compression equipment as part of the BoP especially in power-to-gas (P2G) applications and in industrial processes requiring high pressure hydrogen. In energy-storage (ES) applications including hydrogen-to-power (HtP) with hydrogen stored as compressed hydrogen (CH_2) in vessels or large (seasonal) underground storage facilities, compression equipment (Sdanghi *et al.*, 2020, Durmuş *et al.*, 2021, Tahan, 2022, Marciuš *et al.*, 2022) including electrochemical hydrogen compressors (EHCs) may or may not be part of the BoP of a particular system. EHC can be proton exchange polymer membrane (PEM) based operating at low temperature (< 100 °C) or proton-conducting ceramic (PCC) (4.1.12) based operating at high temperature (550-650 °C) (Kee *et al.*, 2019, Zou *et al.*, 2020, Mushtaq *et al.*, 2022).

In power-to-mobility (P2M) applications with hydrogen stored as liquefied hydrogen (LH_2) in vessels, liquefaction equipment may or may not be part of the BoP of a particular system. Where systems jointly use points of connection (PoCs) for electricity and/or fluid supply as well as for conveying exiting hydrogen as part of a

plant, the system boundary as the delineation between system interior and system exterior should be defined by the manufacturer preferably in agreement with the user.

The application of the testing protocols presented herein do not require specification of the type and characteristics of the test item (**4.1.19**), whether a HTE stack (section 5.1) or a HTSEL system (section 5.2). HTSEL systems operating as rSOEs or rPCEs may comprise stacks of reversible fuel cell (rFC) type in a single device capable of operating in electrolysis mode and fuel cell (FC) mode. Alternatively, systems may comprise two types of separate stacks operating as electrolyser and FC, respectively.

2 Objective and scope of this document

The objective of this document is to present testing protocols (section 6) for establishing the performance (4.1.10) including efficiency and durability (4.1.4) of HTE stacks and the reliability (4.1.14) of HTSEL systems used for generating bulk amounts of hydrogen by high-temperature electrolysis (HTEL) of (pressurised) steam (section 3) at temperature in excess of 550 °C (773,15 K). The stacks and systems (section 5) use electricity preferably from least dispatchable sources of renewable energy (solar, wave, wind, etc) as well as available (waste) heat. HTSEL systems may be deployed in various applications where hydrogen is used as an energy carrier (fuel or commodity) among others in ES such as P2G, P2M (road, rail, maritime) and power-to-X (P2X) including power-to-chemical (P2C), power-to-liquid (P2L) and power-to-fuel (P2F), as well as for direct use as feedstock or reductant in H2I processes.

By applying these testing protocols to a test plan (section 6.5), the performance and durability of stacks and the reliability of systems are established under given test conditions (section 6.2) ⁽⁹⁾, for example,

- To evaluate R&D progress made,
- To set R&I priorities for development milestones and technological benchmarks to improve technology and assess impact on cost and
- To make well-informed business decisions regarding technology selection of a particular stack or system.

Note, these protocols apply to oxygen ion-conducting solid oxide electrolyzers (O-SOEs) including rSOEs performing SOEL and hydrogen ion (proton) conducting solid oxide electrolyzers (H-SOEs) also known as PCE including rPCEs performing PCCEL.

The test methods suggested are mainly those contained in standards of ISO and IEC ⁽¹⁰⁾. Readers are advised to sufficiently familiarise with the referred standards and the test methods described or cited therein.

In addition, we also consider testing procedures previously developed by FCH2JU funded research projects ⁽¹¹⁾ particularly MultiPLHY (CEA, 2020), REFLEX (CEA, 2018), GAMER (SINTEF, 2018) and SOCTESQA (DLR, 2014, Lang *et al.*, 2019) as well as those resulting from the EU electrolysis harmonisation activities (Malkow and Pilenga, 2023). The present document is not intended to exclude any other related testing procedures or test methods.

The operation profiles presented (section 6.7) serve as examples to establish primarily the durability of HTE stacks as well as the reliability of HTSEL systems. They can be complemented by duty cycles, for example, to reflect realistic RES power profiles for on-demand stack operation including the performance of services especially to balance renewable energy loads on the electricity grid (grid balancing services) ⁽¹²⁾.

The estimation of durability serves to assess performance degradation, for example, measured as a positive rate of change in stack voltage (section 6.8.4) and to predict remaining useful life (RUL) and maintenance needs of HTE stacks and HTSEL systems.

These generic protocols constitute testing guidance including mandatory requirements and agreed reference operating conditions for HTE stacks (SOE and PCE) to establish the performance and durability of stacks and the reliability of HTSEL systems in a given P2H2 application. They also allow sufficient flexibility when the test plan (section 6.5) of a scheduled test campaign is drawn up. Thus, the test plan is to provide further details on

- test execution including
 - setting of test input parameters (TIPs) (4.1.20) with permissible variations,
 - test criteria and
 - operation profile(s)

based on the stated purpose(s) and objective(s) of the tests and

- where necessary, provide more specific details on
 - test set-up (*e.g.* gas pre-heater, furnace including temperature distribution, sensor positions, pneumatic/mechanical stack compression, etc)
 - testing procedures including start-up and shut-down,
 - instrumentation and measurement methods,

⁽⁹⁾ Note, the key performance indicator (KPI) targets of the SRIA state for SOEL technologies atmospheric pressure of hydrogen at a purity of 5 (99,999 vol-% of hydrogen in the yielded product gas), see online the notes at https://www.clean-hydrogen.europa.eu/knowledge-management/sria-key-performance-indicators-kpis_en.

⁽¹⁰⁾ These standards can be purchased directly from ISO and IEC or their constituting national committees.

⁽¹¹⁾ These documents (Aicart *et al.*, 2020, Graves *et al.*, 2018, Vøllestad *et al.*, 2018, Malkow *et al.*, 2014) are available for download.

⁽¹²⁾ Working group (WG) 32 of ISO Technical Committee (TC) 197 currently prepares the approved working item (AWI) entitled "ISO 22734-2 Hydrogen generators using water electrolysis - Industrial, commercial, and residential applications - Part 2: Testing guidance for performing electricity grid service".

- data acquisition (DAQ) and
- post-processing of test results including an agreed set of test output parameters (TOPs) (**4.1.21**).

Users of this document may selectively execute tests that are suitable for the objective(s) and purpose(s) of their test campaign from those described herein.

3 Overview of high-temperature steam electrolysis technologies

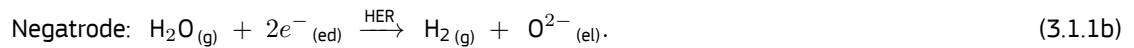
3.1 High-temperature steam electrolysis electrode reactions

For the generation of one mole of gaseous (denoted by subscript _(g)) hydrogen ($H_{2(g)}$) along with half a mole of gaseous oxygen ($O_{2(g)}$) by HTSEL of one mole of water vapour ($H_2O_{(g)}$), the two known HTE technologies are

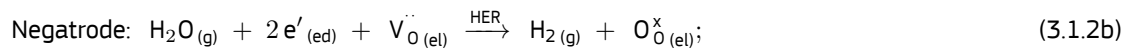
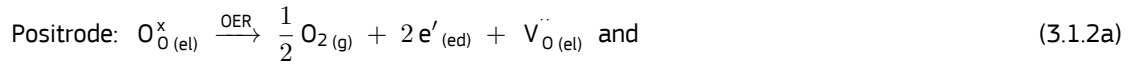
- **SOE** where oxygen is formed by oxidising oxygen ions (O^{2-}) at the positive electrode, air/oxygen electrode or positrode in the oxygen evolution reaction (OER):



under a positive difference in potential (voltage) in excess of the open circuit voltage (OCV). This difference is the result of the supplied direct current (DC) or applied DC voltage. Simultaneously at the negative electrode, hydrogen/fuel electrode or negatrode, gaseous hydrogen is formed by reducing water vapour (steam) in the hydrogen evolution reaction (HER):

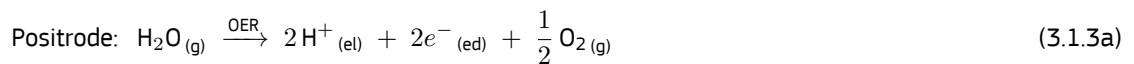


The electrons (e^{-}) are conducted via the electrodes (denoted by subscript _(ed)) connected to an external circuit (DC power supply) entailing an ohmic resistance. The oxygen ions diffuse under the potential difference along grain boundaries (two-dimensional crystalline planar defects between lattices of different crystalline orientation) and via doubly positively charged oxygen ion lattice vacancies ($V_{O}^{\bullet\bullet}$) through the grains (lattices with same crystal orientation) of the polycrystalline oxide ceramic electrolyte membrane (denoted by subscript _(el)) of the SOC (**4.1.15**). This entails an additive ionic resistance. In Kröger–Vink notation (Kröger and Vink, 1956, Kröger and Vink, 1958), the electrode reactions (3.1.1) read



O^{\times}_{O} and e' denote neutral oxygen ion lattice site and electron in the lattice, respectively. Note, in a rSOE operated in FC mode also known as solid oxide fuel cell (SOFC) mode, the electrode reactions (3.1.1) proceed in reverse direction from right to left (of the OER/HER arrow) by drawing current. That is, the reverse of reaction (3.1.1a) is the oxygen reduction reaction (ORR) at the FC cathode (positive electrode) to generate oxygen ions while the reverse of reaction (3.1.1b) is the hydrogen oxidation reaction (HOR) at the FC anode (negative electrode) to generate water vapour. The SOFC cathode (positive electrode) is the SOEC positrode and the SOFC anode (negative electrode) is the SOEC negatrode. In SOFC mode also heat is produced, while in SOEC mode, a rSOE like an ordinary SOE consumes heat when operated below the temperature-dependent thermal-neutral voltage (U_{tn})⁽¹³⁾ and produces heat when operated above this voltage. Heat removal from stacks is primarily by the flow of sweep gas (**4.1.18**) typically air or oxygen when dilution with air is to be avoided.

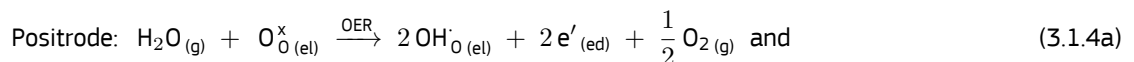
- **PCE** where oxygen is formed by oxidising water vapour (steam) at the positrode in the OER:



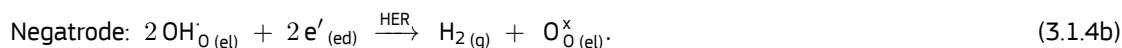
under an applied DC potential (DC voltage) in excess of the OCV. Gaseous hydrogen is simultaneously formed by reducing protons (H^{+}) at the negatrode in the HER:



Whereas electrons are conducted via the electrodes connected to an external circuit, protons are conducted mainly by Grotthuss-type diffusion (proton hopping) via protonic defects such as hydroxide ions at singly positively charged oxygen ion lattice sites (OH^{\bullet}_{O}) through the electrolyte membrane of the PCC made of disordered or sub-stoichiometric oxides (Duan *et al.*, 2020). In Kröger–Vink notation, the electrode reactions (3.1.3) read



⁽¹³⁾ At standard ambient pressure ($p^0 = 100$ kPa) and standard ambient temperature ($T^0 = 298,15$ °C), the thermal-neutral voltage is 1,481 V while this voltage is 1.286 V at 800 °C.



Note, in a rPCE operated in FC mode also known as proton-conducting ceramic fuel cell (PCFC) mode, the electrode reactions (3.1.3) proceed in reverse direction from right to left (of the OER/HER arrow) by drawing current. That is, the reverse of reaction (3.1.3a) is the ORR at the FC cathode (positive electrode) to generate water vapour while the reverse of reaction (3.1.3b) is the HOR at the FC anode (negative electrode) to generate protons. The PCFC cathode (positive electrode) is the PCEC positrodde and the PCFC anode (negative electrode) is the PCEC negatrodde. In PCFC mode also heat is produced, while in PCEC mode, a rPCE like an ordinary PCE consumes heat when operated below the thermal-neutral voltage and produces heat when operated above this voltage. In the latter case, the heat is removed from the stack primarily by steam as sweep gas.

Remark, the OCV of a HTE stack, whether of type SOE or type PCE, is only measurable reliably in the presence of the respective reactants concomitant on the two electrodes in sufficient quantities.

3.2 Materials, configurations and technology readiness levels

Whereas rSOE have to-date obtained technology readiness level (TRL) 5 at most (Bianchi and Bosio, 2021), SOEs with SOEC as constituting units are most mature with TRL 6 at present (Bianchi and Bosio, 2021) benefiting from decades of SOFC research. Least mature with TRL lower than 5 are PCEs which are currently at the early development phase including research for suitable stack design and manufacturing processes as well as research for most suitable combinations of electrode and electrolyte materials for PCECs as constituting units.

Most common in SOECs are yttria-stabilised zirconia (YSZ) as electrolyte, strontium-doped lanthanum cobalt iron oxide (LSCF) or strontium-doped lanthanum cobalt oxide (LSC) with and without ceria-doped gadolinium oxide (CGO) as positrodde and Ni-cermet as negatrodde.

SOEC/PCEC geometries can be tubular or planar. Planar SOECs/PCECs may be circular, square or rectangular. The mechanical support of planar SOECs/PCECs may be provided by one of the electrodes, the electrolyte or a (porous) metal interconnect⁽¹⁴⁾. For planar SOECs/PCECs, the interconnect acts simultaneously as current collector. The geometry of planar HTE stacks being assemblies of several cells sandwiched between gas flow channel-containing interconnects which are electrically connected in series, is usually rectangular or square.

Note, monolithic is a less common stack geometry. Stacks comprising various tubular cells bundled together in parallel arrangement are also possible. Likewise, they are electrically connected using metallic interconnects.

3.3 Operation modes of HTE stacks

Under galvanostatic conditions, input current is provided to the HTE stack resulting in a voltage for each cell making up the voltage of the stack when all cells are electrically connected in series. Under potentiostatic conditions, an input voltage is applied to the stack resulting in a current flowing through the stack perpendicular to the active electrode area (**4.1.3**) (A_{act}) of the SOECs/PCECs. Depending on the supplied current and alternatively, the applied voltage as well as the input temperature primarily of steam transferring heat to the HTE stack, the stack is operated endothermic, isothermal or exothermic. The operation mode of the stack affects both, the energy efficiency (**4.1.6**) (η_e) and its degradation in performance. Performance degradation results in voltage increase under galvanostatic conditions. It occurs with accumulated hours of stack operation whether or not continuous. In addition, it occurs with high and varying input power to the stack. The three operation modes of a HTE stack are

- *Endothermic operation:* The steam temperature decreases from input to output of the stack with its voltage below the thermal-neutral voltage. Among all three modes of operation, this corresponds to the highest energy efficiency of the stack (section 6.6.13). But, it comes at the expensive of a low hydrogen output rate (section 6.6.8). The heat required for the HTSEL reactions (3.1.1) and (3.1.3) to proceed as desired stems under presumed adiabatic conditions mainly from that of the supplied gases especially steam rather than from ohmic (Joule) heating due to an insufficient supply of electricity (current or voltage).
- *Isothermal (thermal-neutral) operation:* The steam temperature is virtually the same at both, input and output of the stack with its voltage basically kept at the thermal-neutral voltage. The energy efficiency of the stack is better than under exothermic operation but this efficiency increase is often outweighed by higher cost. The additional heat required to sustain the equilibrium of the HTSEL reactions (3.1.1) and (3.1.3) usually stems from Joule heating due to the externally supplied electricity which is also required to establish the

⁽¹⁴⁾ In metal-supported cells (MSCs), porous metal supports, whether or not suitably coated, are used to facilitate gas transport especially in PCE which operate at lower temperatures than SOE. Thereby, PCEs are often less prone to excessive degradation by oxidation when in operation. Materials related degradation by oxidation is exhibited, in particular, by reduced pore size and lower electrical conductivity due to the formation of metal oxide(s).

reversible potential (U_{rev})⁽¹⁵⁾. Given the difference in voltage between the thermal-neutral voltage and the reversible potential (voltage) at operating temperature and pressure of a HTE stack, Joule heating in stacks can beneficially be replaced by an extra amount of heat supplied to the stack when available⁽¹⁶⁾. This is especially true for (waste) heat, for example, from energy conversion and other industrial processes where heat is generated by other means than employing electricity. It is also applicable to heat stemming from natural resources such as geothermal and solar energy. Given the same electricity input to a HTSEL system, the utilisation of high-temperature heat in HTE stacks is the reason why hydrogen generation by HTSEL can be more energy efficient when compared to LTWE with the same hydrogen output rate and quality (section 6.6.8).

- *Exothermic operation:* The steam temperature increases from input to output of the stack with its voltage above the thermal-neutral voltage. As a result, the energy efficiency of the stack is the lowest among all three operation modes. This is because more heat is generated by Joule heating due to the supplied electricity in this mode than what is actually required to sustain the HTSEL reactions (3.1.1) and (3.1.3). An advantage of this mode is that the more electricity is supplied to the stack, the higher its hydrogen output rate is. It comes on the expense of an increase in performance degradation. That is, a voltage limit of rarely more than 2.2 V per cell is usually applied in operation under potentiostatic conditions and galvanostatic conditions⁽¹⁷⁾ alike to prevent excessive stack degradation. At system level, the heat generated by the stack can be recovered to boost the energy efficiency.

⁽¹⁵⁾ At standard ambient pressure and temperature, the reversible potential is 1,230 V while this potential is 0,978 V at 800 °C.

⁽¹⁶⁾ The amount of heat (continuously) available along with the steam pressure and temperature will usually determine the dimension (size, input power range, hydrogen output rate), configuration and technology of the HTE stack(s) to be used in a HTSEL system.

⁽¹⁷⁾ for stack operation under quasi-potentiostatic conditions, see section 6.2

4 Terminology

Terms and definitions used in this document are given below as well as in two JRC reports (Tsotridis and Pilenga, 2018, Malkow *et al.*, 2021). In addition, ISO and IEC maintain terminological databases at the following websites:

- ISO Online browsing platform available at <https://www.iso.org/obp>.
- IEC Electropedia available at <http://www.electropedia.org>.

The verbal forms used have the following meaning:

- “shall” indicates a requirement,
- “should” indicates a recommendation,
- “may” indicates a permission and
- “can” indicates a possibility or a capability.

Reference to Système International d’Unités (SI) coherent (derived) units includes, as appropriate, metric prefixes of the concerned unit. Following clause 9.1 of ISO/IEC Directives, Part 2 (ISO and IEC, 2021), decimal fractions are denoted by comma. Alongside SI units, non-SI units may be used as customary. For example, degree Celsius ($^{\circ}\text{C}$) is used as unit of temperature (T) alongside Kelvin (K) and kilo Watt hours (kWh) is used as unit of energy (E) instead of kilo Joule (kJ).

4.1 Terms and definitions

4.1.1 accelerated lifetime testing (ALT)

destructive testing of an item by subjecting it to aggravated conditions (*e.g.* pressure, temperature, voltage, etc) in excess of nominal conditions of real-life use, in an attempt to reveal faults and modes of failure in a short amount of time and to assess the item’s RUL mainly for commercial purposes

4.1.2 accelerated stress testing (AST)

testing of an item by applying high levels of stress when operated (*e.g.* pressure, temperature, voltage, etc) for a short amount of time in an attempt to trigger the same performance degradation mechanism(s) as would presumably occur for a longer exposure of the item when tested under normal conditions of use; it is intentionally non-destructive and mainly for identifying potentially detrimental operating conditions and modes of operation as well as unsuitable designs and ineffective materials

4.1.3 active electrode area (A_{act})

geometric area of the electrode perpendicular to the direction of the current flow

[Source: IEV 485-02-08]

Note 1 to entry: Active electrode area is expressed in cm^2 .

4.1.4 durability

ability of a test item to maintain its performance characteristics as required until the end of RUL, under given conditions of use and maintenance

4.1.5 durability test

test intended to verify whether, or to evaluate to which degree, a test item is able to maintain its performance characteristics over a period of use

4.1.6 energy efficiency (η_e)

ratio of useful energy output to the total energy input including all parasitic and auxiliary energy needed to operate the system

Note 1 to entry: Energy efficiency is expressed in %.

4.1.7 Faradaic (current) efficiency (η_F)

fraction of the electric current passing through an electrochemical cell which accomplishes the desired chemical reaction

[Source: IEV 114-03-07]

Note 1 to entry: Faradaic efficiency is expressed in %.

4.1.8 flexibility

ability of a test item to operate variably, that is, to ramp-up and/or ramp-down its output rapidly in response to a change in input

4.1.9 hydrogen output conditions

specified conditions of pressure of hydrogen (p_{H_2}) and temperature of hydrogen (T_{H_2})

4.1.10 performance characteristics

characteristics defining the ability of a test item to operate as required, under given conditions of use and maintenance

4.1.11 performance test

test intended to verify whether, or to evaluate to which degree, a test item is able to accomplish its performance characteristics

4.1.12 proton-conducting ceramic (PCC)

(sub-stoichiometric) ceramic membrane enabling bulk conduction of protons (H^+)

4.1.13 reactivity

time taken (t_{resp}) by a test item in response to a change in input

4.1.14 reliability

ability of a test item to adequately perform as required, without failure, for a specified time (t), under given conditions of use and maintenance

4.1.15 solid oxide cell (SOC)

electrochemical cell that uses an ion-conducting oxide as the electrolyte

4.1.16 standard ambient temperature and pressure (SATP) conditions

standard ambient pressure ($p^0 = 100$ kPa) and standard ambient temperature ($T^0 = 298,15$ K)

4.1.17 steam conversion (SC)

ratio of number of water molecules converted into hydrogen in the product gas on output to the total number of water molecules on input

4.1.18 sweep gas

inlet stream of gas used to remove heat from a high-temperature electrolyser stack

Note 1 to entry: Sweep gas is distinct from flush gas used either to remove unwanted gas from the SOEC/PCEC or for re-oxidation purpose.

Note 2 to entry: Sweep gas is air in SOE and steam in PCE.

4.1.19 test item

high-temperature electrolyser stack or high-temperature steam electrolysis system

4.1.20 test input parameter (TIP)

parameter whose values can be set in order to define the test conditions of the test system including the operating conditions of the test object

Note 1 to entry: TIPs have to be controllable and measurable. Values of TIPs are known before conducting the test. TIPs can be either static or variable. Static TIPs stay constant and variable TIPs are varied during the test.

[Source: IEC 62282-8-101 3.1.33 (IEC, 2020c)]

4.1.21 test output parameter (TOP)

parameter that indicates the response of the test system/test object as a result of variation of test input parameters

[Source: IEC 62282-8-101 3.1.34 (IEC, 2020c)]

Note 1 to entry: Values of TOPs are unknown before conducting the test and will be measured during the test or subsequently be calculated.

4.2 Abbreviations and acronyms used

A list of abbreviations and acronyms used in this report is appended, see page 40.

4.3 Symbols used

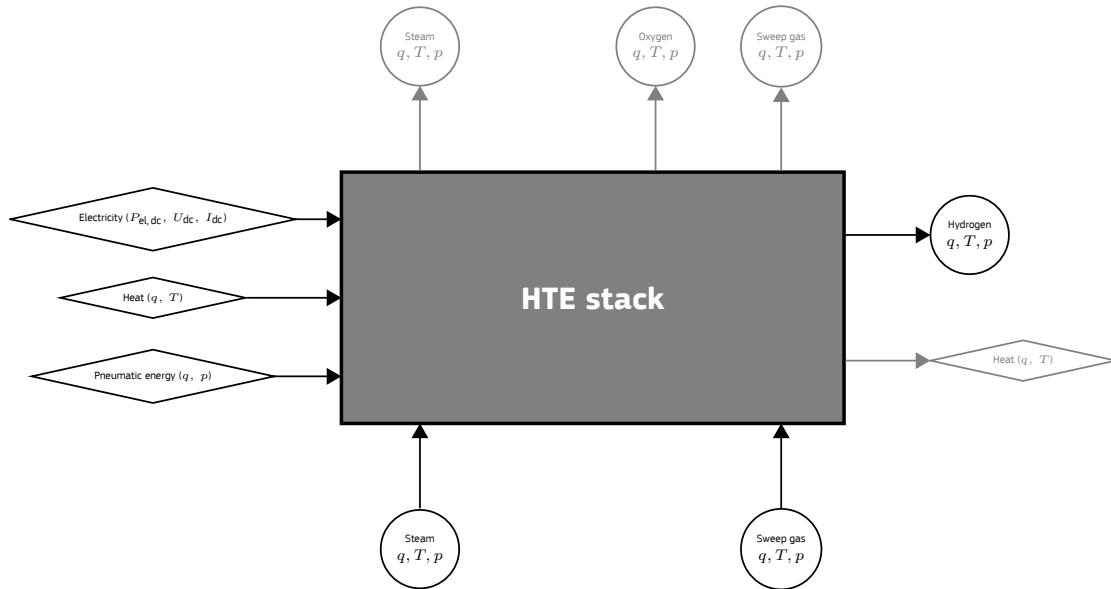
A list of symbols used in this report is appended, see page 43.

5 Description of test items

5.1 HTE stack

Figure 5.1 shows schematically the input and output streams of energy forms and substances of a HTE stack where $P_{el,dc}$, q , p and T stand for DC power ⁽¹⁸⁾, flow rate, pressure and temperature, respectively.

Figure 5.1: Schematic of the input and output streams (directional arrows) of energy forms (diamond shape) and substances (circular shape) of a high-temperature electrolyser stack (rectangular shape). The thick line around the grey shaded box represents the stack boundary.



Source: JRC, 2023.

At its PoCs, the input energy streams to a HTE stack are

- **Electricity** in the form of electric energy:

$$E_{el} \text{ (kWh)} = P_{el} \text{ (kW)} \cdot t \text{ (h)} \text{ where} \quad (5.1.1)$$

P_{el} is electric power and t is the duration during which the electric power is applied. Specifically, the electric power of a stack is DC power:

$$P_{el,dc} \text{ (kW)} = U_{dc} \text{ (kV)} \cdot I_{dc} \text{ (A)}. \quad (5.1.2)$$

- **Heat**, if any, in the form of thermal energy:

$$E_{th} \text{ (kWh)} = P_{th} \text{ (kW)} \cdot t \text{ (h)} \text{ where} \quad (5.1.3)$$

P_{th} is thermal power given by equation (5.1.4) and t is the duration of heat supply.

$$P_{th} \text{ (kW)} = \sum_i q_m^i \text{ (kg/s)} \cdot c_p^i \text{ (kJ/(kg K))} \cdot (T^i \text{ (K)} - T^0 \text{ (K)}); \quad (5.1.4)$$

q_m^i , c_p^i and T^i are mass flow rate, specific heat capacity at constant pressure and temperature of fluid i , respectively. The heat transfer fluids i (input substance streams) are

- typically air or oxygen as sweep gas to SOE and
- steam as feed to SOE ⁽¹⁹⁾ and as feed and sweep gas to PCE.

- **Pneumatic energy** ⁽²⁰⁾:

$$E_{compr} \text{ (kWh)} = P_{compr} \text{ (kW)} \cdot t \text{ (h)} \text{ where} \quad (5.1.5)$$

⁽¹⁸⁾ DC power is calculated according to equation (5.1.2).

⁽¹⁹⁾ The thermal power conveyed by steam to the negatrode is additive to that conveyed by air to the positrode.

⁽²⁰⁾ Pneumatic energy is only relevant for pressurised stacks.

P_{compr} is power of compression given by equation (5.1.6) and t is the duration of pressurised stack operation.

$$P_{\text{compr}} \text{ (kW)} = \sum_j \left(\frac{\gamma^j}{\gamma^j - 1} \right) \frac{\bar{Z}^j \cdot R_g \text{ (kJ/(mol K))} \cdot T^0 \text{ (K)} \cdot q_n^j \text{ (mol/h)} \left(\frac{p^j \text{ (kPa)}}{p^0 \text{ (kPa)}} \right)^{\frac{\gamma^j - 1}{\gamma^j}}}{3600 \text{ (s/h)}}; \quad (5.1.6)$$

R_g , \bar{Z}^j , q_n^j and p^j are universal gas constant, average compressibility factor, molar flow rate and pressure of fluid j , respectively. The isentropic expansion factor of fluid j is

$$\gamma^j = \frac{c_p^j \text{ (kJ/(kg K))}}{c_v^j \text{ (kJ/(kg K))}};$$

c_p^j and c_v^j are specific heat capacity at constant pressure and volume of fluid j , respectively. For a pressurised stack, the pneumatic fluids j (input substance streams) are

- compressed air to SOE ⁽²¹⁾ and
- pressurised steam to SOE and PCE.

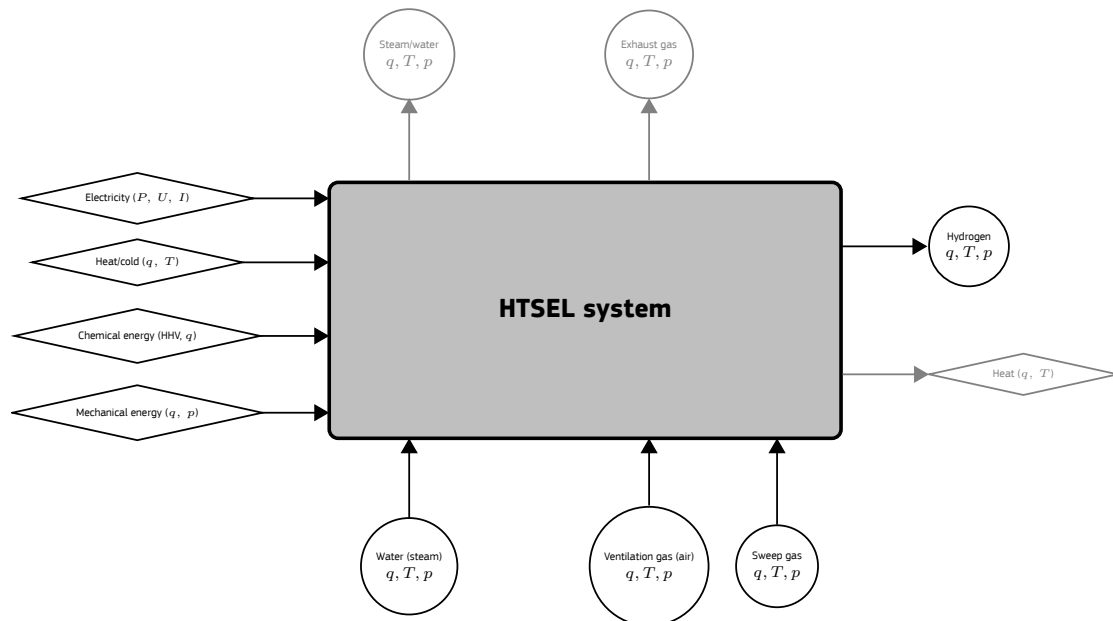
The output streams of the stack are for

- **SOE**
 - **oxygen in sweep gas** (air) at the positrode,
 - **hydrogen in steam** at the negatrode and
 - Heat conveyed by these fluids.
- **PCE**
 - **oxygen in sweep gas** (steam) at the positrode,
 - **hydrogen** at the negatrode and
 - Heat conveyed by these fluids.

5.2 HTSEL system

Figure 5.2 shows schematically the input and output streams of energy forms and substances of a HTSEL system where I , U and P stand for current, voltage and power ⁽²²⁾, respectively.

Figure 5.2: Schematic of the input and output streams (directional arrows) of energy forms (diamond shape) and substances (circular shape) of a high-temperature steam electrolysis system (rectangular shape). The thick line around the grey shaded box represents the system boundary.



Source: JRC, 2023.

⁽²¹⁾ The power of compression conveyed by air to the positrode is additive to that conveyed by steam to the negatrode.

⁽²²⁾ AC power and DC power are calculated according to equation (5.2.1) and equation (5.1.2), respectively.

At its PoCs, the input energy streams to a HTSEL system are

- **Electricity** in the form of electric energy, see equation (5.1.1) using
 - DC power, see equation (5.1.2),
 - AC power ($P_{el,ac}$) whether symmetrical three-phase AC power:

$$P_{el,3p,ac} \text{ (kW)} = \sqrt{3} \cdot U_{ac} \text{ (kV)} \cdot I_{ac} \text{ (A)} \cdot \cos \varphi \quad (5.2.1a)$$

or single-phase AC power:

$$P_{el,1p,ac} \text{ (kW)} = U_{ac} \text{ (kV)} \cdot I_{ac} \text{ (A)} \cdot \cos \varphi; \quad (5.2.1b)$$

U_{ac} , I_{ac} and $\cos \varphi$ are respectively the root-mean-square (rms) AC voltage, rms alternating current and power factor (IEEE, 2010), or

- both, AC power and DC power.
- **Heat/cold**, if any, in the form of thermal energy, see equation (5.1.3), carried by fluids i (input substance streams). For example, heat may be used to heat up water to generate steam while cold may be used to cool down the generated hydrogen and oxygen gases.
- **Chemical energy**, if any, represented by the higher heating value (HHV) of gaseous fuel (HHV^f) with molar flow rate (q_n^f); for example, natural gas (NG) may be used to generate steam from water (H_2O) ⁽²³⁾ in which case equation (5.1.4) reads

$$P_{th} \text{ (kW)} = \text{HHV}^f \text{ (kWh/mol)} \cdot q_n^f \text{ (mol/h)} + \sum_i q_m^i \text{ (kg/s)} \cdot c_p^i \text{ (kJ/(kg K))} \cdot (T^i \text{ (K)} - T^0 \text{ (K)}). \quad (5.2.2)$$

- **Mechanical energy**, if any, in the form of hydraulic energy conveyed, for example, by hydraulic oil and in the form of pneumatic energy, see equation (5.1.5), for example conveyed by compressed air, pressurised steam, or both. For example, stack compression may require hydraulic fluids, control devices may be actuated by compressed air and substances (steam, hydrogen or oxygen) may be compressed by supplied hydraulic fluid(s) or pneumatic fluid(s) as input substance streams ⁽²⁴⁾.

The output streams of the system are

- **Hydrogen**,
- **Water/steam**,
- **Oxygen** in sweep gas (air for SOE and steam for PCE) ⁽²⁵⁾,
- Heat conveyed by these fluids and
- Exhaust gas mainly ventilation off-gas and carbon dioxide, for example, when NG is used as fuel to generate steam.

⁽²³⁾ Instead of NG, systems may generate steam from water using electricity or supplied heat.

⁽²⁴⁾ Hydraulic energy and pneumatic energy are additive for the system especially for systems using pressurised HTE stacks.

⁽²⁵⁾ Although often used, sweep gas (air) is optional.

6 Testing protocols

6.1 General

The operation of the test items, whether a HTE stack (Figure 5.1) or a HTSEL system (Figure 5.2), shall be in accordance with applicable safety requirements (Annex A) and the manufacturer's instructions.

The testing of the stack or system under given test conditions (section 6.2) consists of executing, usually at their beginning-of-life (BoL) ⁽²⁶⁾, all or selected types of performance tests (**4.1.11**) according to a defined test plan (section 6.5) depending on the purpose(s) and objective(s) of the test campaign.

Note, the purpose of a test campaign could be establishing the performance and/or durability of a stack or the reliability of a system in a given application whether for assessing research progress, advancing product development or technology monitoring and assessment (TMA). The objective of a test campaign could be to determine under which conditions and modes of operation defined KPIs may or may not be achieved by the stack or system in the target application.

For example, at a given input current (I_{in}) or input voltage (U_{in}), hydrogen output rate also known as molar flow rate of hydrogen (q_{n,H_2}) calculated by equation (6.6.1), the area-specific resistance (ASR) (R_{ASR}) calculated by equation (6.6.11) (de Marco *et al.*, 2017) and for PCE, the Faradaic (current) efficiency (**4.1.7**) (η_F) calculated by equation (6.6.13) may be chosen as KPIs for HTE stacks subject to performance tests. For systems, the hydrogen output rate, the specific energy consumption (ε_e), the specific electric energy consumption (ε_{el}) and the specific thermal energy consumption (ε_{th}) may be chosen as KPIs at a given input power (P_{in}) according to the purpose(s) and objective(s) of the test campaign, see section 6.8.4 for KPIs regarding durability.

In a test campaign, performance tests (section 6.6) of a stack or system at BoL are usually followed by durability tests (section 6.8) conducted either at constant power, constant current or constant voltage for a prescribed period of use of the stack or system (section 6.8.2), or by employing application-oriented operation profiles (section 6.7) as appropriate for the intended use of the stack or system (section 6.8.3).

As an option, performance tests may intermittently be executed at specified intervals to assess how the stack or system has maintained or altered its performance characteristics ⁽²⁷⁾. This also applies to the end of the test campaign when the final degree of the ability of the stack or system to maintain its performance characteristics is evaluated and alterations thereof are determined (section 6.8.4). Also, the test plan (section 6.5) may require to regularly perform safety checks (Annex A) on the stack and/or system. Testing shall not be continued for stacks and systems which are unsafe to operate.

The hydrogen output conditions (**4.1.9**) of the stack(s) and system including permissible variations shall be defined prior to testing and recorded in the test report (Annex C).

The change(s) in the performance characteristics are usually also graphically presented versus the total test duration or the number of performed operation profiles or sequence(s) of operation profiles (section 7).

Guidance on how to carry out an uncertainty analysis of the test results is provided by the Guide to the expression of uncertainty in measurement (GUM) (JCGM, 2009).

6.2 Test conditions

The test conditions including any permissible variation are

- The environmental conditions of the immediate surrounding (ambient) of the item under test such as air (composition, velocity, pressure, temperature, humidity), salinity, ultraviolet (UV) radiation and other (weather) conditions, see also clause 4.4 of IEC 60204-1:2016+AMD1:2021 CSV (IEC, 2021).
- The actual operating conditions and operation mode(s) including start-up, normal operation, shut-down and quiescence (standby).

They shall be defined prior to testing in accordance with the purpose(s) and objective(s) of the test campaign and be in conformity with the specification of the stack or system as provided by the manufacturer.

Note, the TIPs used in the various performance and durability tests shall be based on these operating conditions and modes of stack or system operation. In the test plan (section 6.5), the individual set values of these TIPs shall be listed per test along with the related TOPs (test results) whether measured or calculated.

Remark, while electrode gas feed compositions are TIPs to be set, the electrode gas pressures and the stack temperature are TOPs needing regulation. Other reference operating conditions can be the manufacturer specified rated stack power (P_{stack}), rated stack current (I_{stack}) or rated stack voltage (U_{stack}).

In the first case, the stack power is a TIP to be set while stack current and voltage are measured TOPs. In the second case, stack current is the TIP to be set and stack voltage is a measured TOP while stack power is a

⁽²⁶⁾ For a stack, BoL shall be the start of first-time operation following complete conditioning according to manufacture's instructions.

⁽²⁷⁾ Note, the operation regime applied to the stack during a performance test can affect its degradation.

calculated (derived) TOP. In the third case, stack voltage is the TIP to be set and stack current is a measured TOP while stack power is again a calculated (derived) TOP.

A special case is thermal-neutral stack operation (section 3.3). In this case, the stack voltage initially set to thermal-neutral voltage for the anticipated stack temperature is a TIP and the stack current at beginning-of-test (BoT) is a TOP along with the measured stack temperature. Then, the stack is operated under galvanostatic conditions using the stack current measured at BoT as TIP while the voltage of the stack becomes a TOP. Upon observing within a prescribed margin a voltage increase due to degradation of the stack given its continued operation, the stack temperature is regularly increased in order to compensate the degradation of the stack. As a result, the stack voltage reduces to the level of the thermal-neutral voltage at the initial stack temperature. This procedure is followed until the maximum operating temperature of the stack recommended by the manufacturer is reached. Subsequently, the current of the stack must be lowered to compensate any further stack degradation exhibited by continuing increases in voltage. The operation of the stack under such conditions can be described as quasi-potentiostatic conditions (Aicart *et al.*, 2020).

6.3 Reference test conditions

Reference test conditions may be agreed prior to testing to facilitate comparison of test results. Exemplary, Table 6.1 provides reference operating conditions recommended for typical HTE stacks of type SOE and PCE.

Table 6.1: Recommended reference operating conditions for typical HTE stacks

Description	Symbol (unit)	SOE ⁽¹⁾	PCE ⁽²⁾
Positrode gauge outlet pressure	p^{pos} (kPa)	100 (± 2 %)	100 (± 2 %)
Negatrode gauge outlet pressure	p^{neg} (kPa)	100 (± 2 %)	100 (± 2 %)
Positrode gas feed composition ⁽³⁾	$p^{\text{H}_2\text{O}}/p^{\text{O}_2}$ (kPa/kPa)	-	0,75 (± 2 %)/0,25 (± 2 %)
Negatrode gas feed composition ⁽³⁾	$p^{\text{H}_2\text{O}}/p^{\text{H}_2}$ (kPa/kPa)	0,9 (± 2 %)/0,1 (± 2 %)	-
Stack temperature ⁽⁴⁾	T_{stack} (K)	973,15 (± 2 K) ⁽⁵⁾	873,15 (± 2 K)

Note: The test plan (section 6.5) may list other reference operating conditions.

⁽¹⁾ including rSOE when operated in electrolysis mode

⁽²⁾ including rPCE when operated in electrolysis mode

⁽³⁾ Inert gas additions (*e.g.* argon) are permitted, for example, to obtain a higher than ambient outlet pressure; $p^{\text{H}_2\text{O}}$, p^{O_2} and p^{H_2} are the partial pressures of water vapour, oxygen and hydrogen, respectively.

⁽⁴⁾ Unless otherwise agreed, the sensor position(s) to determine the stack temperature should be specified by the manufacturer (*e.g.* top of the stack if inlet and outlet gases are supplied and exit from the bottom of the stack; otherwise, in the center of the stack). In the absence of knowledge on sensor position, the average between the inlet and outlet gas temperatures may be regarded as the stack temperature.

⁽⁵⁾ The stack temperature may be different for SOC of type cathode-supported cell (CSC) where the tick and porous negatrode provides mechanical support to the SOC and of type electrolyte-supported cell (ESC) where this support is provided by the somewhat thicker dense electrolyte. Usually, SOCs of type ESC operate at a higher temperature up to 100 K more than those of type CSC.

Source: JRC, 2023

When agreed, the stack or system should first be subject to testing employing such reference test conditions before proceeding to their testing under other specified test conditions. For example, clause 5.2.3.1 of ISO 22734:2019 (ISO, 2019) mentions common environmental conditions as reference test conditions. For SOEL technologies, the SRIA states as KPI target atmospheric pressure of hydrogen at a purity of 5 which is 99,999 vol-% of hydrogen in the yielded product gas (see online at https://www.clean-hydrogen.europa.eu/knowledge-management/sria-key-performance-indicators-kpis_en).

6.4 Measurement techniques

The test equipment, measuring instruments and measurement methods shall conform to the relevant standard (*e.g.* IEC 61010-1:2010+AMD1:2016 CSV (IEC, 2016)), test method or testing procedure employed. Instruments shall be calibrated in accordance with the applicable standard(s), measurement method(s) or procedure(s) recommended by the manufacturer of the stack or system to meet the targeted uncertainties of the concerned test parameters whether TIPs or TOPs. The measurement set-up employed shall be documented in the test report (Annex C). Also, available calibration records and certificates of the measuring instruments should likewise be documented to be available on request.

6.5 Test plan

For a test item, the test plan shall be drawn up taking into account

- (a) the item's specification and manufacturer's instructions (*e.g.* for the stack: maximum pressure and temperature, range of heating/cooling rates and electrode gas compositions, etc),
- (b) the test conditions (section 6.2),
- (c) the measurement techniques and instrumentation (section 6.4),
- (d) test type (section 6.6 and section 6.8), sequence, frequency and duration,
- (e) the DAQ including number, permissible range and logging rate of the data points ⁽²⁸⁾,
- (f) the state of calibration of the measuring instruments,
- (g) post-processing of test results including data reduction and uncertainty analysis in accordance with the GUM (JCGM, 2009),
- (h) one or more KPIs, whether measured or derived TOPs, as a result of performance tests (**4.1.11**) and
- (i) one or more test stop criteria to (prematurely) end testing for preventing unintended failure or destruction.

One or more KPIs shall be defined to assess the performance and durability of the test item. For this purpose, TIPs and TOPs should be specified to obtain KPIs as functions of such parameters. For example, these parameters are, but should not be limited to,

1. the input electric power ($P_{el,in}$) (section 6.6.1) whether
 - AC power or
 - DC power,
2. the input current whether
 - alternating current or
 - direct current,
3. the input voltage whether
 - AC voltage or
 - DC voltage,
4. the pressure of hydrogen (p_{H_2}),
5. the temperature of hydrogen (T_{H_2}),
6. the stack temperature (T_{stack}),
7. the steam conversion (SC) (**4.1.17**) calculated by equation (6.6.12) and
8. the gas feed composition to the electrodes.

Tests may also be conducted at environmental conditions other than standard ambient temperature and pressure (SATP) conditions; for example, system start-up and shut-down may be established for an ambient pressure (p) different to standard ambient pressure and an ambient temperature (T) below or above standard ambient temperature to simulate conditions likely to be experienced at different installation sites.

Consistent with the purpose(s) and objective(s) of the test campaign, the test plan should specify the test methods and measurement techniques to be employed where standards, testing procedures and manufacturer's instructions provide for different possibilities. It may also list (micro-structural) characterisation methods, for example, to perform post-test analysis of the stack for gaining more insight into the obtained test results.

6.6 Performance tests

6.6.1 Input electric power

The input electric power to a HTE stack or HTSEL system shall be determined in accordance with clause 5.2.1 of ISO 16110-2:2010 (ISO, 2010).

⁽²⁸⁾ Considering the duration of the individual tests and the expected standard uncertainty in the measurements, different numbers, ranges and data logging rates may be chosen for the various performance tests (section 6.6) and the durability tests (section 6.8).

6.6.2 Input thermal power

The input thermal power ($P_{th,in}$) to a HTE stack or HTSEL system conveyed by heat transfer fluid(s) shall be determined in accordance with clause 5.2.2.1 of ISO 16110-2:2010 (ISO, 2010).

6.6.3 Input power of compression

The input power of compression ($P_{comp,in}$) to a HTE stack or HTSEL system conveyed by hydraulic/pneumatic fluid(s), if any, shall be determined in accordance with clause 5.2.2.1 of ISO 16110-2:2010 (ISO, 2010).

6.6.4 Start-up time and energy

The start-up time (t_{on}) of a HTSEL system to its rated hydrogen output rate (section 6.6.8) shall be determined in accordance with clause 5.6.1 of IEC 62282-8-201:2020 (IEC, 2020d) for positive ramp (heating) rate (\dot{T}_{heat}) consistent with the manufacturer's instructions. The heating rate is part of the test conditions (section 6.2).

System start-up is usually from cold state, commonly under SATP conditions. The test plan (section 6.5) may also foresee system start-up from a defined hot state (standby).

The start-up energy (E_{on}) may also be determined in accordance with clause 14.5.4.2 of IEC 62282-3-201:2017+AMD1:2022 CSV (IEC, 2022) where reference to FC shall by analogy be replaced by HTSEL.

6.6.5 Response time and ramp energy

The response time (t_{resp}) of a HTSEL system to a given positive or negative ramp rate of a TIP shall be determined in accordance with clause 5.6.1 of IEC 62282-8-201:2020 (IEC, 2020d). Consistent with the manufacturer's instructions, the TIP may be input power, input current or input voltage (see section 6.5).

In the test report (Annex C), the response time in relation to either of these TIPs shall be recorded separately. The same shall apply to the response time for positive and negative ramp rates.

In addition to the response time, the test plan may request to determine the ramp energy (E_{ramp}) for positive and/or negative ramps of the concerned TIP in accordance with clause 14.6.3.2 of IEC 62282-3-201:2017+AMD1:2022 CSV (IEC, 2022) where reference to FC shall by analogy be replaced by HTSEL.

In the test report, the ramp energy for positive and negative ramps shall be recorded separately.

Accordingly, the test plan should specify a set of symbols for response time and ramp energy, for example, by adding appropriate indices to both, response time and ramp energy allowing to differentiate between positive and negative ramp rates.

6.6.6 Shut-down time and energy

The shut-down time (t_{off}) of a HTSEL system shall be determined in accordance with clause 5.6.1 of IEC 62282-8-201:2020 (IEC, 2020d) for negative ramp (cooling) rate (\dot{T}_{cool}) consistent with the manufacturer's instructions. The cooling rate is part of the test conditions (section 6.2).

In addition to the shut-down time, the test plan (section 6.5) may request to determine the shut-down energy (E_{off}) in accordance with clause 14.9.3.2 of IEC 62282-3-201:2017+AMD1:2022 CSV (IEC, 2022) where reference to FC shall by analogy be replaced by HTSEL.

6.6.7 Switch-over time

For rSOE and rPCE, consistent with the manufacturer's instructions, the switch-over time (t_{switch}) of a HTSEL system to switch from FC mode to electrolysis mode and *vice versa* shall be determined in accordance with clause 5.7 of IEC 62282-8-201:2020 (IEC, 2020d).

In the test report (Annex C), the switch-over time for switching from FC mode to electrolysis mode and from electrolysis mode to FC mode shall be recorded. Also, the sequence of switching whether from FC mode to electrolysis mode or from electrolysis mode to FC mode shall be recorded in the test report.

Accordingly, the test plan (section 6.5) should specify, for example, appropriate indices to be added to t_{switch} to differentiate between the two modes and the sequence of switching.

6.6.8 Hydrogen output rate and quality

The product gas output rate also known as product gas molar flow rate ($q_{n,out}$) of a HTE stack or HTSEL system shall be determined in accordance with clause 5.2.11.1 of ISO 22734:2019 (ISO, 2019). From the product gas

molar flow rate, the hydrogen output rate also known as molar flow rate of hydrogen shall be calculated as follows

$$q_{n,H_2} \text{ (mol/h)} = x_{n,H_2} \text{ (mol/mol)} \cdot q_{n,out} \text{ (mol/h)}; \quad (6.6.1)$$

x_{n,H_2} is the molar concentration of hydrogen in the product gas to be determined by gas analysis in accordance with clause 5.2.2.2 of ISO 16110-2:2010 (ISO, 2010). When a H_2O/H_2 mixture is used as negatode gas in a SOE, the molar concentration of hydrogen in such mixture at the input shall be subtracted from that at the output. From the molar flow rate of hydrogen, the volumetric flow rate of hydrogen (q_{v,H_2}) related to SATP conditions is calculated as follows

$$q_{v,H_2} \text{ (m}^3\text{/h)} = q_{n,H_2} \text{ (mol/h)} \cdot V_{m,H_2} \text{ (m}^3\text{/mol)}; \quad (6.6.2)$$

$V_{m,H_2} \approx 24,79 \cdot 10^{-3} \text{ m}^3\text{/mol}$ is the molar volume of hydrogen under SATP conditions. The hydrogen output quality of a HTE stack and HTSEL system other than the molar concentration of hydrogen in the product gas, in particular, humidity shall be determined in accordance with clause 5.2.11.2 of ISO 22734:2019 (ISO, 2019).

6.6.9 Oxygen output rate and quality

The oxygen output rate or molar flow rate of oxygen (q_{n,O_2}) of a HTE stack and HTSEL system shall be determined in accordance with clause 5.2.11.1 of ISO 22734:2019 (ISO, 2019). The oxygen output quality, in particular, the molar concentration of oxygen (x_{n,O_2}) in the sweep gas shall be determined in accordance with clause 5.2.11.2 of ISO 22734:2019 (ISO, 2019). When air is used as sweep gas in SOE, the molar concentration of oxygen in air at the input shall be subtracted from that at the output. When a H_2O/O_2 mixture is used as positrode gas in a PCE, the molar concentration of oxygen in such mixture at the input shall be subtracted from that at the output.

6.6.10 Polarisation curve measurements

The measurement of the current-voltage characteristics ($I_{dc}-U_{dc}$ curves), known as polarisation curves, shall be determined for HTE stacks by applying the Solid Oxide Cell and Stack Testing, Safety and Quality Assurance (SOCTESQA) Test Module (TM) 03 on current-voltage characteristics (de Marco *et al.*, 2017) or in accordance with clause 7.2 of IEC 62282-8-101:2020 (IEC, 2020c). The stack temperature (T_{stack}) shall be recorded as an additional TOP. Its average and maximum should be plotted versus the average of the stack direct current to check for temperature stability during the measurement. Note the maximum stack temperature may be used as an indicator for possible thermal-mechanical stresses in and the stability of the glass sealing of the stack.

From the $I_{dc}-U_{dc}$ curves, the current-electric power characteristics ($I_{dc}-P_{el}$ curves) of the stack may be derived by calculating its electric power ($P_{el,stack}$) given by equation (5.1.2). The electric power density of the stack ($P_{el,d,stack}$) is calculated as follows

$$P_{el,d,stack} \text{ (kW/cm}^2\text{)} = U_{dc} \text{ (kV)} \cdot J_{dc} \text{ (A/cm}^2\text{)} \text{ where} \quad (6.6.3)$$

$$J_{dc} \text{ (A/cm}^2\text{)} = \frac{I_{dc} \text{ (A)}}{A_{act} \text{ (cm}^2\text{)}} \quad (6.6.4)$$

is the current density of the stack; the active electrode area is specified by the manufacturer.

6.6.11 Electrochemical imittance spectroscopy measurements

The electrical impedance (Z)⁽²⁹⁾ and/or electrical admittance ($Y=Z^{-1}$)⁽³⁰⁾ of individual cells in a HTE stack shall be determined by applying the SOCTESQA TM 04 on electrochemical imittance spectroscopy (EIS) (Lang *et al.*, 2017) or in accordance with clause 7.6 of IEC 62282-8-101:2020 (IEC, 2020c). Guidance on EIS measurements is provided by clause 10.7.2.2 of IEC 62282-7-2:2014 (IEC, 2014b) and clause 6.3.10 of IEC 62282-8-101:2020 (IEC, 2020c) while guidance on data-post processing of EIS data is provided by clause 7.6.3 of IEC 62282-8-101:2020 (IEC, 2020c). Useful software tools to perform data-post processing of EIS data are listed in term 403 on p. 66 (online version) of the recently published electrolysis terminology document (Malkov *et al.*, 2021).

From the EIS measurements, the ohmic resistance (R_{Ω}) and the polarisation resistance (R_{pol}) are estimated. In principle, the ohmic resistance is the high-frequency resistance (R_{∞}) that is the electrical impedance at high perturbation frequencies ($f \rightarrow \infty$) with vanishing reactance, $\Im m Z [f \rightarrow \infty] = 0$,

$$\lim_{f \rightarrow \infty} \Re Z [f] \text{ (}\Omega\text{)} = R_{\infty} \text{ (}\Omega\text{)}. \quad (6.6.5)$$

⁽²⁹⁾ The output of EIS measurements conducted under potentiostatic conditions is electrical impedance.

⁽³⁰⁾ The output of EIS measurements conducted under galvanostatic conditions is electrical admittance.

Practically, the high-frequency resistance is taken as the electrical impedance measured at the highest of the probed perturbation frequencies (f_{\max}) where $\Im m Z [f \rightarrow f_{\max}] \rightarrow 0$,

$$\lim_{f \rightarrow f_{\max}} \Re e Z [f] (\Omega) \approx R_{\Omega} (\Omega) \quad (6.6.6)$$

constituting the ohmic resistance (R_{Ω}). The polarisation resistance is the difference between the zero-frequency resistance (R_0) and the high-frequency resistance,

$$R_{\text{pol}} (\Omega) = R_0 (\Omega) - R_{\infty} (\Omega). \quad (6.6.7)$$

The zero-frequency resistance is the electrical impedance at low perturbation frequencies ($f \rightarrow 0$) with vanishing reactance, $\Im m Z [f \rightarrow 0] = 0$,

$$\lim_{f \rightarrow 0} \Re e Z [f] (\Omega) = R_0 (\Omega). \quad (6.6.8)$$

Practically, the zero-frequency resistance is taken as the electrical impedance measured at the lowest of the probed perturbation frequencies (f_{\min}) where $\Im m Z [f \rightarrow f_{\min}] \rightarrow 0$,

$$\lim_{f \rightarrow f_{\min}} \Re e Z [f] (\Omega) \approx R_{\text{lf}} (\Omega) \quad (6.6.9)$$

constituting the low-frequency resistance (R_{lf}). Consequently, the polarisation resistance is approximated as the difference between the low-frequency resistance and the ohmic resistance,

$$R_{\text{pol}} (\Omega) \approx R_{\text{lf}} (\Omega) - R_{\Omega} (\Omega). \quad (6.6.10)$$

The area-specific resistance is calculated as follows

$$R_{\text{ASR}} (\text{m}\Omega \cdot \text{cm}^2) = R_{\text{lf}} (\Omega) \cdot A_{\text{act}} (\text{cm}^2) \cdot 1000 \text{ m}\Omega/\Omega. \quad (6.6.11)$$

In case EIS measurements and polarisation curve measurements (section 6.6.10) are conducted simultaneously, care should be taken in data post-processing of the test results as both, current and voltage, would contain AC and DC contributions.

6.6.12 Specific energy consumption

Under SATP conditions, the specific energy consumption per unit volume of hydrogen ($\varepsilon_{\text{e,v}}$), the specific energy consumption per unit mass of hydrogen ($\varepsilon_{\text{e,m}}$), the specific electric energy consumption per unit volume of hydrogen ($\varepsilon_{\text{el,v}}$) and the specific electric energy consumption per unit mass of hydrogen ($\varepsilon_{\text{el,m}}$) shall be determined for HTSEL systems applying the recently published energy performance testing procedure (Malkow and Pilenga, 2023) which defines these four TOPs ⁽³¹⁾. For systems supplied with heat, the specific thermal energy consumption per unit volume of hydrogen ($\varepsilon_{\text{th,v}}$) and the specific thermal energy consumption per unit mass of hydrogen ($\varepsilon_{\text{th,m}}$) shall be determined applying the same procedure which also defines these two TOPs ⁽³²⁾.

6.6.13 Efficiency

For a HTSEL system, under SATP conditions, the energy efficiency based on the HHV of hydrogen ($\eta_{\text{HHV,e}}^0$), the energy efficiency based on the lower heating value (LHV) of hydrogen ($\eta_{\text{LHV,e}}^0$), the electrical efficiency based on the HHV of hydrogen ($\eta_{\text{HHV,el}}^0$) and the electrical efficiency based on the LHV of hydrogen ($\eta_{\text{LHV,el}}^0$) should be determined applying the recently published energy performance testing procedure (Malkow and Pilenga, 2023) which defines these four TOPs ⁽³³⁾. In addition, the steam conversion of a HTE stack is calculated as follows

$$\text{SC} (\%) = \frac{q_{\text{V,H}_2} (\text{m}^3/\text{h})}{q_{\text{V,H}_2\text{O}} (\text{m}^3/\text{h})} \cdot 100 (\%) = \frac{I_{\text{stack}} (\text{A}) \cdot N_{\text{cells}}}{q_{\text{V,H}_2\text{O}} (\text{m}^3/\text{h})} \cdot \frac{V_{\text{m}} (\text{m}^3/\text{mol}) \cdot 3600 (\text{s/h})}{2F (\text{C/mol})} \cdot 100 (\%); \quad (6.6.12)$$

$q_{\text{V,H}_2}$ is the volumetric flow rate of hydrogen related to SATP conditions on output given by equation (6.6.2), $q_{\text{V,H}_2\text{O}}$ is the volumetric flow rate of steam fed on input, I_{stack} is the stack current, N_{cells} is the number of cells in the stack electrically connected in series, $F = 96485,3 \text{ C/mol}$ is Faraday constant and $V_{\text{m}} = 22,414 \text{ m}^3/\text{mol}$ is the molar volume of ideal gas (hydrogen). The factor 2 in equation (6.6.12) stems from the fact that two

⁽³¹⁾ Therein, see equations (3.2.1) and (3.2.9).

⁽³²⁾ Therein, see equation (3.2.10).

⁽³³⁾ Therein, see equations (3.2.11) and (3.2.12).

electrons are exchanged in the electrode reactions (3.1.1) and (3.1.3). For a PCE, the Faradaic efficiency (³⁴) given by

$$\eta_F (\%) = \frac{2F (\text{C/mol}) \cdot q_{n,\text{H}_2} (\text{mol/s})}{I (\text{A})} \cdot 100 (\%), \quad (6.6.13)$$

should also be determined; F is the Faraday constant, I is the externally supplied current and q_{n,H_2} is given by equation (6.6.1). The factor 2 in equation (6.6.13) stems from the fact that two electrons are exchanged in the PCEC electrode reactions (3.1.3).

6.7 Operation profiles

6.7.1 General

Operation profiles, whether profiles of the input electric power, input current or input voltage versus time (t), are intended to simulate, under given test conditions (section 6.2), the operation of the stack or system for use in the application concerned. This includes real-world operation profiles (duty cycles) derived from RES-based power profiles typical for the intermittent supply of power to a HTSEL system by various RES types. The derived duty cycle may be expressed in terms of input electric power or translated into input current using a typical value of rated voltage or translated into input voltage using a typical value of rated current. The time interval of a profile (cycle) is usually a fixed period comprising the time required to carry out a given number of consecutive profiles (cycles) of the same type or a sequence of profiles (cycles) of different types according to the test plan (section 6.5). Thus, individual profiles (cycles) may constitute building blocks of a test sequence (³⁵).

6.7.2 Graphical representation

Figure 6.1 shows the graphical representation of an idealised operation profile (normalised set point versus profile duration) as building block for a sequence of operation profiles to test the reactivity (**4.1.13**) of a stack or system (Tsotridis and Pilenga, 2021). Similarly, Figure 6.2, Figure 6.3 and Figure 6.4 show the graphical representation of idealised operation profiles as building blocks for sequences of operation profiles to test the flexibility (**4.1.8**) of a stack or system (Tsotridis and Pilenga, 2021). The operation profile presented in Figure 6.2 simulates high flexibility while the operation profiles presented in Figure 6.3 and Figure 6.4 simulate flexibility limited to 100 % and 200 % of the normalised set point, respectively. The reactivity operation profile is meant to simulate severe conditions in terms of set ramp rate(s) and frequency of change in the set point while the three flexibility operation profiles are meant to simulate at different degrees frequent periods of variation in the set point (Tsotridis and Pilenga, 2021).

For both, reactivity and flexibility, the total duration taken per completed profile to (positive and negative) ramps should be determined (section 6.6.5) and recorded in the test report (Annex C). They may graphically be presented to show their evolution versus the total sequence(s) of the performed operation profiles and/or the number of operation profiles or sequence(s) of operation profiles performed. According to the test plan (section 6.5), the normalised set point as displayed in Figure 6.1 to Figure 6.4 is the ratio of either

- the specified input electric power to its nominal (rated) value ($P_{\text{el, nom}}$) specified by the manufacturer namely

$$\text{Normalised electric power set point (\%)} = \frac{P_{\text{el, in}} (\text{kW})}{P_{\text{el, nom}} (\text{kW})} \cdot 100 \%,$$

- the specified input current to its nominal (rated) value (I_{nom}) specified by the manufacturer namely

$$\text{Normalised current set point (\%)} = \frac{I_{\text{in}} (\text{A})}{I_{\text{nom}} (\text{A})} \cdot 100 \% \text{ or}$$

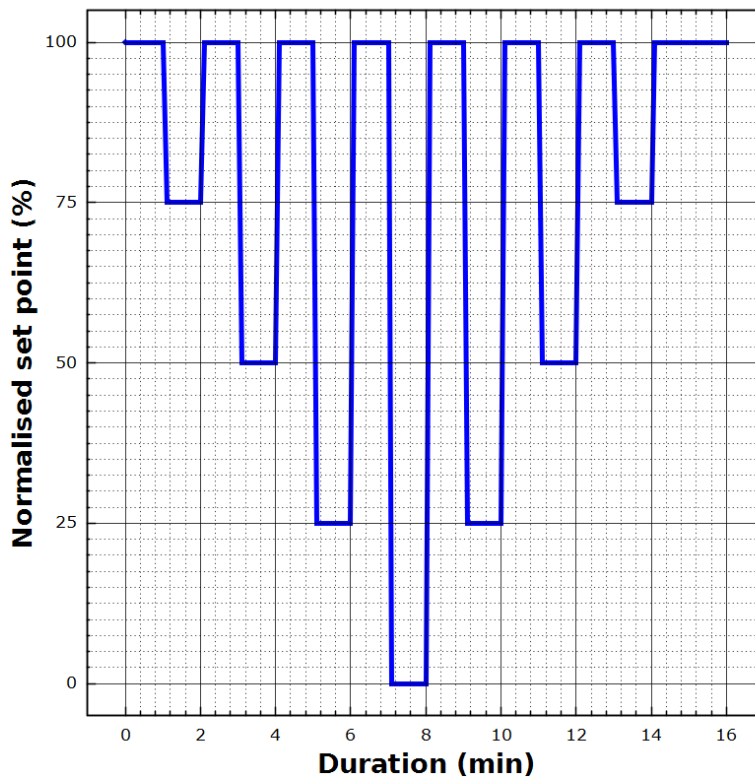
- the specified input voltage to its nominal (rated) value (U_{nom}) specified by the manufacturer namely

$$\text{Normalised voltage set point (\%)} = \frac{U_{\text{in}} (\text{kV})}{U_{\text{nom}} (\text{kV})} \cdot 100 \%.$$

⁽³⁴⁾ Remark, as most PCCs in PCECs are mixed ionic and electronic conductors (MIECs), commonly acceptor doped barium zirconate (BaZrO_3) and barium cerate (BaCeO_3), electronic leakage occurs usually via small polarons (M_{V}^{\bullet}) and electron holes (h^{\bullet}) resulting in a reduced proton flux and thus, a lower hydrogen flow. As a result, the Faradaic efficiency is less than 100 %.

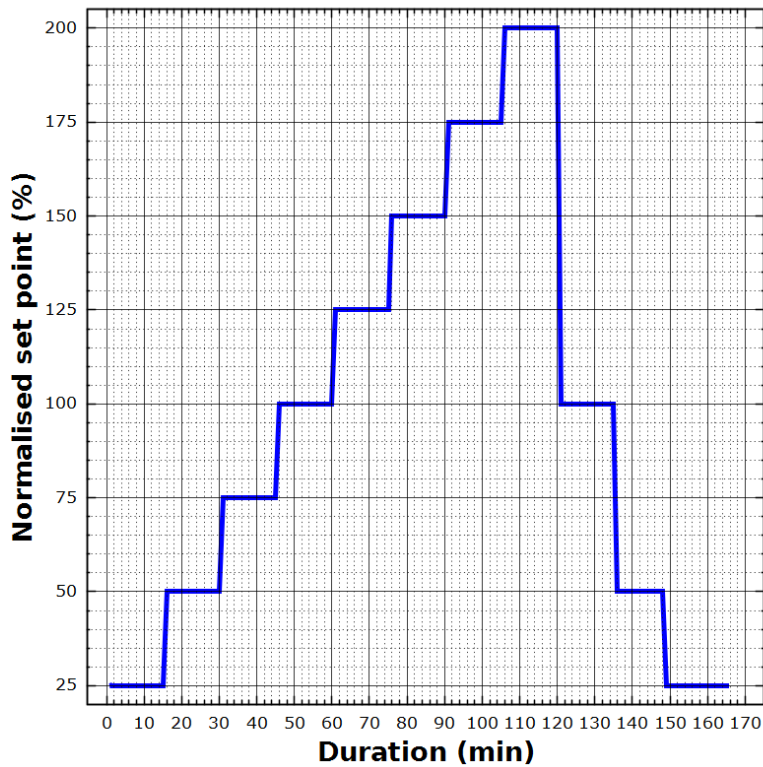
⁽³⁵⁾ Operation profiles for rSOE may include periods of alternating operation in SOEC mode and SOFC mode (Graves *et al.*, 2018). Likewise, operation profiles for rPCE may include periods of alternating operation in PCEC mode and PCFC mode. In such case, the test plan (section 6.5) should provide details on switching between electrolysis mode and FC mode while also addressing safety concerns (Annex A), especially regarding high voltages and pressures, formation or release of harmful gases and occurrence of hot surfaces, as well as preventing excessive stack degradation or damage and sustained system dysfunction or failure.

Figure 6.1: Graph of an idealised operation profile (normalised set point versus profile duration) for testing the reactivity of a stack or system (Table B.1).



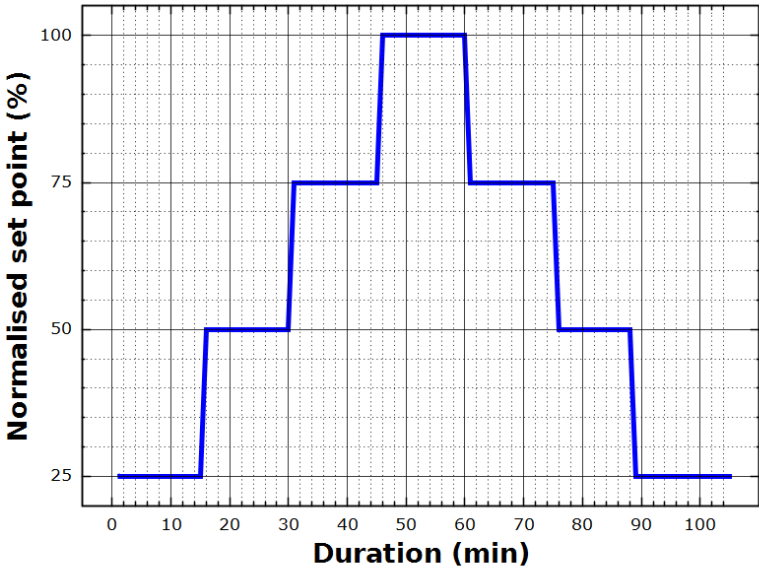
Source: JRC, 2022.

Figure 6.2: Graph of an idealised operation profile (normalised set point versus profile duration) for testing the high flexibility of a stack or system (Table B.2).



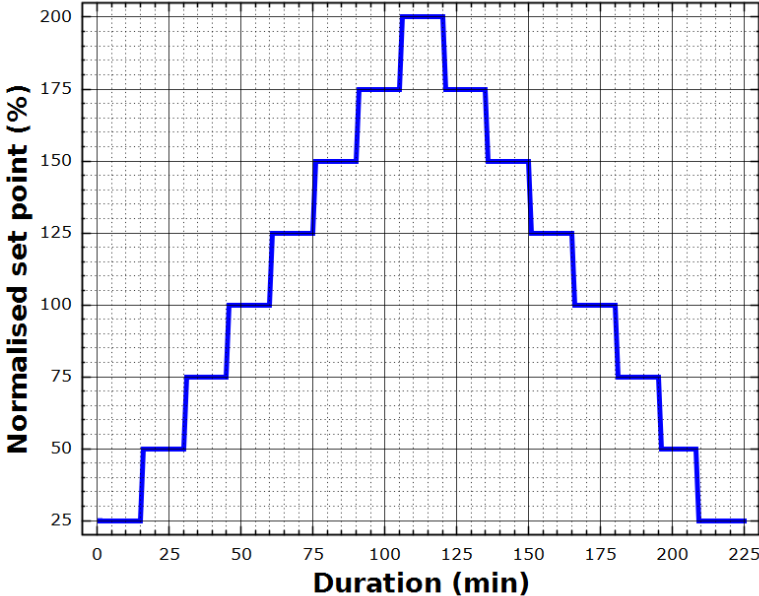
Source: JRC, 2022.

Figure 6.3: Graph of an idealised operation profile (normalised set point versus profile duration) for testing 100 % flexibility of a stack or system (Table B.3).



Source: JRC, 2022.

Figure 6.4: Graph of an idealised operation profile (normalised set point versus profile duration) for testing 200 % flexibility of a stack or system (Table B.4).



Source: JRC, 2022.

Note, the operation profiles displayed in Figure 6.2 and Figure 6.4 shall only be applied where the specification of the stack or system by the manufacturer allow operation at 200 % of rated power, current or voltage as appropriate ⁽³⁶⁾. Annex B contains the tabulated data of each of these operation profiles.

6.8 Durability tests

6.8.1 General

Durability tests (4.1.5) on HTE stacks evaluate the ability of the stack to maintain its performance characteristics under specified test conditions (section 6.2) for a given time interval ⁽³⁷⁾ when subjected to testing either at constant “steady-state” operation (section 6.8.2) or variable operation (section 6.8.3) applying one or more operation profiles (section 6.7). The two operation modes may also be combined. For example, they may be applied alternately or applied in a specified sequence typical for a stack in a given application. Preferably, the duration of each interval *k* comprises one thousand or more hours of stack operation.

For HTSEL systems, durability tests evaluate the ability of the system to maintain its reliability (4.1.14) under specified test conditions (section 6.2) for a given time interval ⁽³⁸⁾ when subjected to testing either at constant “steady-state” operation or variable operation applying one or more operation profiles (section 6.7) or indeed, duty cycles. Similar to HTE stacks, the two operation modes may be combined. For example, alternately or by a specified sequence typical for the intended use of the system in a given application. Preferably, the duration of each interval *k* comprises one thousand or more hours of system operation.

In addition to performance tests at BoT and end-of-test (EoT), performance tests (section 6.6) may, as an option, be conducted intermittently at intervals (*k*=1,2,...) in accordance with the test plan to determine one or more KPIs. Importantly, BoT should not be BoL for a stack. The stack should have been operated for a sufficient long period as recommended by the manufacturer but at least for 1000 hours in order to overcome the phase of possible initial high degradation common after operating the stack for the first time ⁽³⁹⁾.

The inability of a stack to maintain its performance characteristics during testing in accordance with a specified stop criterion may be regarded as stack failure. Also, the inability of a system to perform as required during testing in accordance with a specified stop criterion may be regarded as a reliability failure of the system.

6.8.2 Constant stack operation

Durability testing of a HTE stack under constant power, constant current or constant voltage shall be conducted in accordance with clause 7.4 of IEC 62282-8-101:2020 (IEC, 2020c).

6.8.3 Variable stack operation

Durability testing of a HTE stack under variable power, variable current or variable voltage using operation profiles (section 6.7) or indeed, duty cycles derived from RES power profiles shall be conducted in accordance with clause 7.7 of IEC 62282-8-101:2020 (IEC, 2020c).

6.8.4 KPI estimation

For a specified stack current (I_{stack}) or stack current density (J_{stack}), the durability of the stack at an elapsed time interval t_k is assessed from the difference (deviation) of the stack voltage at that instant, $U(t_k)$ and at t_0 , $U(t_0)$, by calculating the total rate of change of voltage ($\Delta_{tot}^k U$) whether positive (degradation) or negative (improvement) ⁽⁴⁰⁾ as follows

$$\Delta_{tot}^k U (\mu V/h) = \frac{U(t_k) (kV) - U(t_0) (kV)}{t_k (h) - t_0 (h)} \cdot 10^9 \mu V/kV; \quad (6.8.1)$$

t_k is the time elapsed from BoT at t_0 until the time at the end of interval *k* whether for constant stack operation (section 6.8.2) or variable stack operation (section 6.8.3). At both instants (t_0 and t_k), the stack voltages may be determined as average values from polarisation curve measurements (section 6.6.10) conducted in electrolysis mode under galvanostatic conditions ⁽⁴¹⁾. In the absence of test results from polarisation curve measurements,

⁽³⁶⁾ Similar considerations apply when real-world operation profiles are used as actual duty cycles in durability tests (section 6.8).

⁽³⁷⁾ It may comprise a specified duration or the time required to complete a specified number of operation profiles (duty cycles) or a specified sequence of operation profiles (duty cycles).

⁽³⁸⁾ see footnote 37

⁽³⁹⁾ A system manufacturer may have similar recommendations for the first time use of one or another BoP component.

⁽⁴⁰⁾ For a rSOE operated in SOFC mode and a rPCE operated in PCFC mode, a positive total rate of change of voltage represents improvement while a negative total rate of change of voltage represents degradation when assessing the average values of stack voltage in polarisation curve measurements conducted in FC mode under galvanostatic conditions.

⁽⁴¹⁾ Average values of stack voltage for use in equation (6.8.1) and equation (6.8.2) can only be determined by polarisation curve measurements when the stack was operated under quasi-potentiostatic conditions (section 6.2).

the average value of the stack voltage at the end of interval k shall be determined from the stack voltage values recorded during the durability test ⁽⁴²⁾. A minimum of three consecutive data points including the actual stack voltage at t_k shall be taken to calculate this average value. More than three data points should be used when the estimated standard uncertainty for the calculated average of the stack voltage is considered too large. The relative rate of change of voltage ($\Delta_{\text{rel}}^k U$) corresponding to a minimum of 1000 hours of stack operation is calculated whether positive (degradation) or negative (improvement) as follows (McPhail *et al.*, 2022)

$$\Delta_{\text{rel}}^k U (\%) = \frac{U(t_k) (\text{kV}) - U(t_0) (\text{kV})}{U(t_0) (\text{kV})} \cdot \frac{1000 (\text{h})}{t_k (\text{h})} \cdot 100 \%. \quad (6.8.2)$$

The specified stack current (stack current density) is usually the current (current density) occurring at the thermal-neutral voltage of the stack when operated under given conditions at BoT. According to the test plan (section 6.5), it may also be the current (current density) which occurs at a stack voltage different from the thermal-neutral voltage ⁽⁴³⁾.

Stack durability may also be assessed by means of the area-specific resistance at a specified stack current or stack current density ⁽⁴⁴⁾. Then, the durability of the stack at t_k is assessed from the difference of the area-specific resistance at that instant, $R_{\text{ASR}}(t_k)$ and at t_0 , $R_{\text{ASR}}(t_0)$, by calculating the total rate of change of area-specific resistance ($\Delta_{\text{tot}}^k R_{\text{ASR}}$) whether positive (degradation) or negative (improvement) as follows

$$\Delta_{\text{tot}}^k R_{\text{ASR}} (\text{m}\Omega \text{ cm}^2/\text{h}) = \frac{R_{\text{ASR}}(t_k) (\Omega \text{ cm}^2) - R_{\text{ASR}}(t_0) (\Omega \text{ cm}^2)}{t_k (\text{h}) - t_0 (\text{h})} \cdot 1000 \text{ m}\Omega/\Omega. \quad (6.8.3)$$

At both instants (t_0 and t_k), the ASR values are determined preferably as average values from EIS measurements (section 6.6.11) conducted in electrolysis mode under galvanostatic conditions. The relative rate of change of area-specific resistance ($\Delta_{\text{rel}}^k R_{\text{ASR}}$) corresponding to a minimum of 1000 hours of stack operation is calculated whether positive (degradation) or negative (improvement) as follows (McPhail *et al.*, 2022)

$$\Delta_{\text{rel}}^k R_{\text{ASR}} (\%) = \frac{R_{\text{ASR}}(t_k) (\Omega \text{ cm}^2) - R_{\text{ASR}}(t_0) (\Omega \text{ cm}^2)}{R_{\text{ASR}}(t_0) (\Omega \text{ cm}^2)} \cdot \frac{1000 (\text{h})}{t_k (\text{h})} \cdot 100 \%. \quad (6.8.4)$$

For a specified current (stack current density) of a PCE stack ⁽⁴⁵⁾, the total rate of change of Faradaic efficiency ($\Delta_{\text{tot}}^k \eta_F$) is calculated whether positive (degradation) or negative (improvement) as follows

$$\Delta_{\text{tot}}^k \eta_F (\%/h) = \frac{\eta_F(t_k) (\%) - \eta_F(t_0) (\%)}{t_k (\text{h}) - t_0 (\text{h})}; \quad (6.8.5)$$

$\eta_F(t_k)$ is the Faradaic efficiency at t_k and $\eta_F(t_0)$ is the Faradaic efficiency at t_0 . At both instants (t_0 and t_k), the values of Faradaic efficiency are calculated employing equation (6.6.13). The relative rate of change of Faradaic efficiency ($\Delta_{\text{rel}}^k \eta_F$) corresponding to a minimum of 1000 hours of stack operation is calculated whether positive (degradation) or negative (improvement) as follows

$$\Delta_{\text{rel}}^k \eta_F (\%) = \frac{\eta_F(t_k) (\%) - \eta_F(t_0) (\%)}{\eta_F(t_0) (\%)} \cdot \frac{1000 (\text{h})}{t_k (\text{h})} \cdot 100 \%. \quad (6.8.6)$$

For a specified input power ⁽⁴⁶⁾, the durability of a HTSEL system at an elapsed time interval t_k is assessed from the difference of the specific energy consumption per unit volume of hydrogen ($\varepsilon_{\text{e,v}}$) and the specific energy consumption per unit mass of hydrogen ($\varepsilon_{\text{e,m}}$) at t_k and t_0 by calculating the total rate of change of specific energy consumption per unit volume of hydrogen ($\Delta_{\text{tot}}^k \varepsilon_{\text{e,v}}$) and the total rate of change of specific energy consumption per unit mass of hydrogen of hydrogen ($\Delta_{\text{tot}}^k \varepsilon_{\text{e,m}}$) whether positive (degradation) or negative (improvement) as follows

$$\Delta_{\text{tot}}^k \varepsilon_{\text{e,v}} ((\text{J}/\text{m}^3)/h) = \frac{\varepsilon_{\text{e,v}}(t_k) (\text{kWh}/\text{m}^3) - \varepsilon_{\text{e,v}}(t_0) (\text{kWh}/\text{m}^3)}{t_k (\text{h}) - t_0 (\text{h})} \cdot 3600 \text{ s}/h \cdot 1000 \text{ J}/\text{kJ} \text{ and} \quad (6.8.7a)$$

⁽⁴²⁾ The temperature of the stack operated under quasi-potentiostatic conditions (section 6.2) may, as an option, replace the stack voltage as KPI in equation (6.8.1) and equation (6.8.2). It applies to all intervals where the stack current was not lowered.

⁽⁴³⁾ In case the total rate of change of voltage and the relative rate of change of voltage are determined for more than one value of stack current (stack current density), appropriate indices should be added to $\Delta_{\text{tot}}^k U$ and $\Delta_{\text{rel}}^k U$.

⁽⁴⁴⁾ In case the total rate of change of area-specific resistance and the relative rate of change of area-specific resistance are determined for more than one value of stack current (stack current density), appropriate indices should be added to $\Delta_{\text{tot}}^k R_{\text{ASR}}$ and $\Delta_{\text{rel}}^k R_{\text{ASR}}$.

⁽⁴⁵⁾ In case the total rate of change of Faradaic efficiency and the relative rate of change of Faradaic efficiency are determined for more than one value of stack current, appropriate indices should be added to $\Delta_{\text{tot}}^k \eta_F$ and $\Delta_{\text{rel}}^k \eta_F$.

⁽⁴⁶⁾ In case the total rate of change of specific energy consumption per unit volume of hydrogen, the total rate of change of specific energy consumption per unit mass of hydrogen of hydrogen, the relative rate of change of specific energy consumption per unit volume of hydrogen and the relative rate of change of specific energy consumption per unit mass of hydrogen are determined for more than one value of input power, appropriate indices should be added to $\Delta_{\text{tot}}^k \varepsilon_{\text{e,v}}$, $\Delta_{\text{tot}}^k \varepsilon_{\text{e,m}}$, $\Delta_{\text{rel}}^k \varepsilon_{\text{e,v}}$ and $\Delta_{\text{rel}}^k \varepsilon_{\text{e,m}}$.

$$\Delta_{\text{tot}}^k \varepsilon_{e,m} ((\text{J/kg})/\text{h}) = \frac{\varepsilon_{e,m}(t_k) (\text{kWh/kg}) - \varepsilon_{e,m}(t_0) (\text{kWh/kg})}{t_k (\text{h}) - t_0 (\text{h})} \cdot 3600 \text{ s/h} \cdot 1000 \text{ J/kJ}; \quad (6.8.7b)$$

$\varepsilon_{e,v}(t_k)$ and $\varepsilon_{e,m}(t_k)$ are respectively the specific energy consumption per unit volume of hydrogen and the specific energy consumption per unit mass of hydrogen at t_k while $\varepsilon_{e,v}(t_0)$ and $\varepsilon_{e,m}(t_0)$ are respectively the specific energy consumption per unit volume of hydrogen and the specific energy consumption per unit mass of hydrogen at t_0 . At both instants (t_0 and t_k), the values of specific energy consumption are determined from measurements in accordance with section 6.6.12. The relative rate of change of specific energy consumption per unit volume of hydrogen ($\Delta_{\text{rel}}^k \varepsilon_{e,v}$) and the relative rate of change of specific energy consumption per unit mass of hydrogen ($\Delta_{\text{rel}}^k \varepsilon_{e,m}$) corresponding to a minimum of 1000 hours of system operation are calculated whether positive (degradation) or negative (improvement) as follows

$$\Delta_{\text{rel}}^k \varepsilon_{e,v} (\%) = \frac{\varepsilon_{e,v}(t_k) (\text{kWh/m}^3) - \varepsilon_{e,v}(t_0) (\text{kWh/m}^3)}{\varepsilon_{e,v}(t_0) (\text{kWh/m}^3)} \cdot \frac{1000 (\text{h})}{t_k (\text{h})} \cdot 100 \% \text{ and} \quad (6.8.8a)$$

$$\Delta_{\text{rel}}^k \varepsilon_{e,m} (\%) = \frac{\varepsilon_{e,m}(t_k) (\text{kWh/kg}) - \varepsilon_{e,m}(t_0) (\text{kWh/kg})}{\varepsilon_{e,m}(t_0) (\text{kWh/kg})} \cdot \frac{1000 (\text{h})}{t_k (\text{h})} \cdot 100 \%. \quad (6.8.8b)$$

For a specified input electric power ⁽⁴⁷⁾, the durability of a HTSEL system at the elapsed time interval t_k may also be assessed from the difference of the specific electric energy consumption per unit volume of hydrogen ($\varepsilon_{el,v}$) and the specific electric energy consumption per unit mass of hydrogen ($\varepsilon_{el,m}$) at t_k and t_0 by calculating the total rate of change of specific electric energy consumption per unit volume of hydrogen ($\Delta_{\text{tot}}^k \varepsilon_{el,v}$) and the total rate of change of specific electric energy consumption per unit mass of hydrogen ($\Delta_{\text{tot}}^k \varepsilon_{el,m}$) whether positive (degradation) or negative (improvement) as follows

$$\Delta_{\text{tot}}^k \varepsilon_{el,v} ((\text{J/m}^3)/\text{h}) = \frac{\varepsilon_{el,v}(t_k) (\text{kWh/m}^3) - \varepsilon_{el,v}(t_0) (\text{kWh/m}^3)}{t_k (\text{h}) - t_0 (\text{h})} \cdot 3600 \text{ s/h} \cdot 1000 \text{ J/kJ} \text{ and} \quad (6.8.9a)$$

$$\Delta_{\text{tot}}^k \varepsilon_{el,m} ((\text{J/kg})/\text{h}) = \frac{\varepsilon_{el,m}(t_k) (\text{kWh/kg}) - \varepsilon_{el,m}(t_0) (\text{kWh/kg})}{t_k (\text{h}) - t_0 (\text{h})} \cdot 3600 \text{ s/h} \cdot 1000 \text{ J/kJ}; \quad (6.8.9b)$$

$\varepsilon_{el,v}(t_k)$ and $\varepsilon_{el,m}(t_k)$ are respectively the specific electric energy consumption per unit volume of hydrogen and the specific electric energy consumption per unit mass of hydrogen at t_k while $\varepsilon_{el,v}(t_0)$ and $\varepsilon_{el,m}(t_0)$ are respectively the specific electric energy consumption per unit volume of hydrogen and the specific electric energy consumption per unit mass of hydrogen at t_0 . At both instants (t_0 and t_k), the values of specific electric energy consumption are determined from measurements in accordance with section 6.6.12. The relative rate of change of specific electric energy consumption per unit volume of hydrogen ($\Delta_{\text{rel}}^k \varepsilon_{el,v}$) and the relative rate of change of specific electric energy consumption per unit mass of hydrogen ($\Delta_{\text{rel}}^k \varepsilon_{el,m}$) corresponding to a minimum of 1000 hours of system operation are calculated whether positive (degradation) or negative (improvement) as follows

$$\Delta_{\text{rel}}^k \varepsilon_{el,v} (\%) = \frac{\varepsilon_{el,v}(t_k) (\text{kWh/m}^3) - \varepsilon_{el,v}(t_0) (\text{kWh/m}^3)}{\varepsilon_{el,v}(t_0) (\text{kWh/m}^3)} \cdot \frac{1000 (\text{h})}{t_k (\text{h})} \cdot 100 \% \text{ and} \quad (6.8.10a)$$

$$\Delta_{\text{rel}}^k \varepsilon_{el,m} (\%) = \frac{\varepsilon_{el,m}(t_k) (\text{kWh/kg}) - \varepsilon_{el,m}(t_0) (\text{kWh/kg})}{\varepsilon_{el,m}(t_0) (\text{kWh/kg})} \cdot \frac{1000 (\text{h})}{t_k (\text{h})} \cdot 100 \%. \quad (6.8.10b)$$

For a specified input thermal power ($P_{\text{th,in}}$) ⁽⁴⁸⁾, the durability of a HTSEL system at the elapsed time interval t_k may additionally be assessed from the difference of the specific thermal energy consumption per unit volume of hydrogen ($\varepsilon_{th,v}$) and the specific thermal energy consumption per unit mass of hydrogen ($\varepsilon_{th,m}$) at t_k and t_0 by calculating the total rate of change of specific thermal energy consumption per unit volume of hydrogen ($\Delta_{\text{tot}}^k \varepsilon_{th,v}$) and the total rate of change of specific thermal energy consumption per unit mass of hydrogen ($\Delta_{\text{tot}}^k \varepsilon_{th,m}$) whether positive (degradation) or negative (improvement) as follows

$$\Delta_{\text{tot}}^k \varepsilon_{th,v} ((\text{J/m}^3)/\text{h}) = \frac{\varepsilon_{th,v}(t_k) (\text{kWh/m}^3) - \varepsilon_{th,v}(t_0) (\text{kWh/m}^3)}{t_k (\text{h}) - t_0 (\text{h})} \cdot 3600 \text{ s/h} \cdot 1000 \text{ J/kJ} \text{ and} \quad (6.8.11a)$$

⁽⁴⁷⁾ In case the total rate of change of specific electric energy consumption per unit volume of hydrogen, the total rate of change of specific electric energy consumption per unit mass of hydrogen, the relative rate of change of specific electric energy consumption per unit volume of hydrogen and the relative rate of change of specific electric energy consumption per unit mass of hydrogen are determined for more than one value of input electric power, appropriate indices should be added to $\Delta_{\text{tot}}^k \varepsilon_{el,v}$, $\Delta_{\text{tot}}^k \varepsilon_{el,m}$, $\Delta_{\text{rel}}^k \varepsilon_{el,v}$ and $\Delta_{\text{rel}}^k \varepsilon_{el,m}$.

⁽⁴⁸⁾ In case the total rate of change of specific thermal energy consumption per unit volume of hydrogen, the total rate of change of specific thermal energy consumption per unit mass of hydrogen, the relative rate of change of specific thermal energy consumption per unit volume of hydrogen and the relative rate of change of specific thermal energy consumption per unit mass of hydrogen are determined for more than one value of input thermal power, appropriate indices should be added to $\Delta_{\text{tot}}^k \varepsilon_{th,v}$, $\Delta_{\text{tot}}^k \varepsilon_{th,m}$, $\Delta_{\text{rel}}^k \varepsilon_{th,v}$ and $\Delta_{\text{rel}}^k \varepsilon_{th,m}$.

$$\Delta_{\text{tot}}^k \varepsilon_{\text{th,m}} \text{ ((J/kg)/h)} = \frac{\varepsilon_{\text{th,m}}(t_k) \text{ (kWh/kg)} - \varepsilon_{\text{th,m}}(t_0) \text{ (kWh/kg)}}{t_k \text{ (h)} - t_0 \text{ (h)}} \cdot 3600 \text{ s/h} \cdot 1000 \text{ J/kJ}; \quad (6.8.11b)$$

$\varepsilon_{\text{th,v}}(t_k)$ and $\varepsilon_{\text{th,m}}(t_k)$ are respectively the specific thermal energy consumption per unit volume of hydrogen and the specific thermal energy consumption per unit mass of hydrogen at t_k while $\varepsilon_{\text{th,v}}(t_0)$ and $\varepsilon_{\text{th,m}}(t_0)$ are respectively the specific thermal energy consumption per unit volume of hydrogen and the specific thermal energy consumption per unit mass of hydrogen at t_0 . At both instants (t_0 and t_k), the values of specific thermal energy consumption are determined from measurements in accordance with section 6.6.12. The relative rate of change of specific thermal energy consumption per unit volume of hydrogen ($\Delta_{\text{rel}}^k \varepsilon_{\text{th,v}}$) and the relative rate of change of specific thermal energy consumption per unit mass of hydrogen ($\Delta_{\text{rel}}^k \varepsilon_{\text{th,m}}$) corresponding to a minimum of 1000 hours of system operation are calculated whether positive (degradation) or negative (improvement) as follows

$$\Delta_{\text{rel}}^k \varepsilon_{\text{th,v}} \text{ (%) } = \frac{\varepsilon_{\text{th,v}}(t_k) \text{ (kWh/m}^3\text{)} - \varepsilon_{\text{th,v}}(t_0) \text{ (kWh/m}^3\text{)}}{\varepsilon_{\text{th,v}}(t_0) \text{ (kWh/m}^3\text{)}} \cdot \frac{1000 \text{ (h)}}{t_k \text{ (h)}} \cdot 100 \text{ \%} \text{ and} \quad (6.8.12a)$$

$$\Delta_{\text{rel}}^k \varepsilon_{\text{th,m}} \text{ (%) } = \frac{\varepsilon_{\text{th,m}}(t_k) \text{ (kWh/kg)} - \varepsilon_{\text{th,m}}(t_0) \text{ (kWh/kg)}}{\varepsilon_{\text{th,m}}(t_0) \text{ (kWh/kg)}} \cdot \frac{1000 \text{ (h)}}{t_k \text{ (h)}} \cdot 100 \text{ \%}. \quad (6.8.12b)$$

In addition, the system durability may be assessed by means of the energy efficiency based on HHV under SATP conditions of hydrogen ($\eta_{\text{HHV,e}}^0$) and the energy efficiency based on LHV under SATP conditions of hydrogen ($\eta_{\text{LHV,e}}^0$) at a specified input power (⁴⁹). That is, the durability of the system at t_k is assessed from the difference of the energy efficiency under SATP conditions of hydrogen, whether based on HHV or LHV, at that instant and at t_0 by calculating the total rate of change of energy efficiency based on HHV under SATP conditions of hydrogen ($\Delta_{\text{tot}}^k \eta_{\text{HHV,e}}^0$) and the total rate of change of energy efficiency based on LHV under SATP conditions of hydrogen ($\Delta_{\text{tot}}^k \eta_{\text{LHV,e}}^0$) whether positive (degradation) or negative (improvement) as follows

$$\Delta_{\text{tot}}^k \eta_{\text{HHV,e}}^0 \text{ (%/h)} = \frac{\eta_{\text{HHV,e}}^0(t_k) \text{ (%) } - \eta_{\text{HHV,e}}^0(t_0) \text{ (%)}}{t_k \text{ (h)} - t_0 \text{ (h)}} \text{ and} \quad (6.8.13a)$$

$$\Delta_{\text{tot}}^k \eta_{\text{LHV,e}}^0 \text{ (%/h)} = \frac{\eta_{\text{LHV,e}}^0(t_k) \text{ (%) } - \eta_{\text{LHV,e}}^0(t_0) \text{ (%)}}{t_k \text{ (h)} - t_0 \text{ (h)}}; \quad (6.8.13b)$$

$\eta_{\text{HHV,e}}^0(t_k)$ and $\eta_{\text{LHV,e}}^0(t_k)$ are respectively the energy efficiency based on HHV under SATP conditions of hydrogen and the energy efficiency based on LHV under SATP conditions of hydrogen at t_k while $\eta_{\text{HHV,e}}^0(t_0)$ and $\eta_{\text{LHV,e}}^0(t_0)$ are respectively the energy efficiency based on HHV under SATP conditions of hydrogen and the energy efficiency based on LHV under SATP conditions of hydrogen at t_0 . At both instants (t_0 and t_k), the values of energy efficiency are determined from measurements in accordance with section 6.6.13. The relative rate of change of energy efficiency based on HHV under SATP conditions of hydrogen ($\Delta_{\text{rel}}^k \eta_{\text{HHV,e}}^0$) and the relative rate of change of energy efficiency based on LHV under SATP conditions of hydrogen ($\Delta_{\text{rel}}^k \eta_{\text{LHV,e}}^0$) corresponding to a minimum of 1000 hours of system operation are calculated whether positive (degradation) or negative (improvement) as follows

$$\Delta_{\text{rel}}^k \eta_{\text{HHV,e}}^0 \text{ (%) } = \frac{\eta_{\text{HHV,e}}^0(t_k) \text{ (%) } - \eta_{\text{HHV,e}}^0(t_0) \text{ (%)}}{\eta_{\text{HHV,e}}^0(t_0) \text{ (%)}} \cdot \frac{1000 \text{ (h)}}{t_k \text{ (h)}} \cdot 100 \text{ \%} \text{ and} \quad (6.8.14a)$$

$$\Delta_{\text{rel}}^k \eta_{\text{LHV,e}}^0 \text{ (%) } = \frac{\eta_{\text{LHV,e}}^0(t_k) \text{ (%) } - \eta_{\text{LHV,e}}^0(t_0) \text{ (%)}}{\eta_{\text{LHV,e}}^0(t_0) \text{ (%)}} \cdot \frac{1000 \text{ (h)}}{t_k \text{ (h)}} \cdot 100 \text{ \%}. \quad (6.8.14b)$$

The system durability may also be assessed by means of the electrical efficiency based on HHV under SATP conditions of hydrogen ($\eta_{\text{HHV,el}}^0$) and the electrical efficiency based on LHV under SATP conditions of hydrogen ($\eta_{\text{LHV,el}}^0$) at a specified input electric power (⁵⁰). That is, the durability of the system at t_k is assessed from the difference of the electrical efficiency under SATP conditions of hydrogen, whether based on HHV or LHV, at that instant and at t_0 by calculating the total rate of change of electrical efficiency based on HHV under SATP

⁽⁴⁹⁾ In case the total rate of change of energy efficiency based on HHV under SATP conditions of hydrogen, the total rate of change of energy efficiency based on LHV under SATP conditions of hydrogen, the relative rate of change of energy efficiency based on HHV under SATP conditions of hydrogen and the relative rate of change of energy efficiency based on LHV under SATP conditions of hydrogen are determined for more than one value of input power, appropriate indices should be added to $\Delta_{\text{tot}}^k \eta_{\text{HHV,e}}^0$, $\Delta_{\text{tot}}^k \eta_{\text{LHV,e}}^0$, $\Delta_{\text{rel}}^k \eta_{\text{HHV,e}}^0$ and $\Delta_{\text{rel}}^k \eta_{\text{LHV,e}}^0$.

⁽⁵⁰⁾ In case the total rate of change of electrical efficiency based on HHV under SATP conditions of hydrogen, the total rate of change of electrical efficiency based on LHV under SATP conditions of hydrogen, the relative rate of change of electrical efficiency based on HHV under SATP conditions of hydrogen and the relative rate of change of electrical efficiency based on LHV under SATP conditions of hydrogen are determined for more than one value of input electric power, appropriate indices should be added to $\Delta_{\text{tot}}^k \eta_{\text{HHV,el}}^0$, $\Delta_{\text{tot}}^k \eta_{\text{LHV,el}}^0$, $\Delta_{\text{rel}}^k \eta_{\text{HHV,el}}^0$ and $\Delta_{\text{rel}}^k \eta_{\text{LHV,el}}^0$.

conditions of hydrogen ($\Delta_{\text{tot}}^k \eta_{\text{HHV,el}}^0$) and the total rate of change of electrical efficiency based on LHV under SATP conditions of hydrogen ($\Delta_{\text{tot}}^k \eta_{\text{LHV,el}}^0$) whether positive (degradation) or negative (improvement) as follows

$$\Delta_{\text{tot}}^k \eta_{\text{HHV,el}}^0 (\%/h) = \frac{\eta_{\text{HHV,el}}^0(t_k) (\%) - \eta_{\text{HHV,el}}^0(t_0) (\%)}{t_k (h) - t_0 (h)} \text{ and} \quad (6.8.15a)$$

$$\Delta_{\text{tot}}^k \eta_{\text{LHV,el}}^0 (\%/h) = \frac{\eta_{\text{LHV,el}}^0(t_k) (\%) - \eta_{\text{LHV,el}}^0(t_0) (\%)}{t_k (h) - t_0 (h)}; \quad (6.8.15b)$$

$\eta_{\text{HHV,el}}^0(t_k)$ and $\eta_{\text{LHV,el}}^0(t_k)$ are respectively the electrical efficiency based on HHV under SATP conditions of hydrogen and the electrical efficiency based on LHV under SATP conditions of hydrogen at t_k while $\eta_{\text{HHV,el}}^0(t_0)$ and $\eta_{\text{LHV,el}}^0(t_0)$ are respectively the electrical efficiency based on HHV under SATP conditions of hydrogen and the electrical efficiency based on LHV under SATP conditions of hydrogen at t_0 . At both instants (t_0 and t_k), the values of electrical efficiency are determined from measurements in accordance with section 6.6.13. The relative rate of change of electrical efficiency based on HHV under SATP conditions of hydrogen ($\Delta_{\text{rel}}^k \eta_{\text{HHV,el}}^0$) and the relative rate of change of electrical efficiency based on LHV under SATP conditions of hydrogen ($\Delta_{\text{rel}}^k \eta_{\text{LHV,el}}^0$) corresponding to a minimum of 1000 hours of system operation are calculated whether positive (degradation) or negative (improvement) as follows

$$\Delta_{\text{rel}}^k \eta_{\text{HHV,el}}^0 (\%) = \frac{\eta_{\text{HHV,el}}^0(t_k) (\%) - \eta_{\text{HHV,el}}^0(t_0) (\%)}{\eta_{\text{HHV,el}}^0(t_0) (\%)} \cdot \frac{1000 (h)}{t_k (h)} \cdot 100 \% \text{ and} \quad (6.8.16a)$$

$$\Delta_{\text{rel}}^k \eta_{\text{LHV,el}}^0 (\%) = \frac{\eta_{\text{LHV,el}}^0(t_k) (\%) - \eta_{\text{LHV,el}}^0(t_0) (\%)}{\eta_{\text{LHV,el}}^0(t_0) (\%)} \cdot \frac{1000 (h)}{t_k (h)} \cdot 100 \%. \quad (6.8.16b)$$

Note, the specified input power (total, electric and/or thermal) is usually the rated power of the system as defined by the manufacturer. According to the test plan (section 6.5), it may also be a fraction or a multiple of the rated power.

7 Presentation of test results

Table 7.1 and Table 7.2 list the TOPs as results of performance tests (section 6.6) and durability tests (section 6.8), respectively.

Table 7.1: Test results of performance tests

Symbol (unit)	Description	Test method
$P_{el,ac,in}$ (kW)	input AC power	6.6.1
$P_{el,dc,in}$ (kW)	input DC power	6.6.1
$P_{th,in}$ (kW)	input thermal power ⁽¹⁾	6.6.2
$P_{compr,in}$ (kW)	input power of compression ⁽²⁾	6.6.3
t_{on} (s)	start-up time	6.6.4
E_{on} (J)	start-up energy	6.6.4
t_{off} (s)	shut-down time	6.6.6
E_{off} (J)	shut-down energy	6.6.6
t_{resp} (s)	response time ⁽³⁾	6.6.5
E_{ramp} (J)	ramp energy ⁽⁴⁾	6.6.5
t_{switch} (s)	switch-over time ⁽⁵⁾	6.6.7
x_{n,H_2} (mol/mol)	product gas molar concentration of hydrogen	6.6.8
q_{n,H_2} (mol/h)	molar flow rate of hydrogen ⁽⁶⁾	6.6.8
q_{V,H_2} (m ³ /h)	volumetric flow rate of hydrogen under SATP conditions ⁽⁶⁾	6.6.8
x_{n,O_2} (mol/mol)	molar concentration of oxygen	6.6.9
q_{n,O_2} (mol/mol)	molar flow rate of oxygen ⁽⁷⁾	6.6.9
I_{stack} (A)	stack current ⁽⁸⁾	6.6.10
J_{stack} (A/cm ²)	stack current density ⁽⁸⁾	6.6.10
U_{stack} (kV)	stack voltage ⁽⁹⁾	6.6.10
$P_{el,stack}$ (kW)	stack electric power	6.6.10
$P_{el,d,stack}$ (kW/cm ²)	stack electric power density	6.6.10
T_{stack} (K)	stack temperature	6.6.10
Z (Ω)	electrical impedance ⁽¹⁰⁾	6.6.11
Y (S)	electrical admittance ⁽¹¹⁾	6.6.11
R_{Ω} (Ω)	ohmic resistance	6.6.11
R_{pol} (Ω)	polarisation resistance	6.6.11
R_{ASR} (m Ω .cm ²)	area-specific resistance	6.6.11
$\varepsilon_{e,v}$ (kWh/m ³)	specific energy consumption per unit volume of hydrogen under SATP conditions	6.6.12
$\varepsilon_{e,m}$ (kWh/kg)	specific energy consumption per unit mass of hydrogen under SATP conditions	6.6.12
$\varepsilon_{el,v}$ (kWh/m ³)	specific electric energy consumption per unit volume of hydrogen under SATP conditions	6.6.12
$\varepsilon_{el,m}$ (kWh/kg)	specific electric energy consumption per unit mass of hydrogen under SATP conditions	6.6.12
$\varepsilon_{th,v}$ (kWh/m ³)	specific thermal energy consumption per unit volume of hydrogen under SATP conditions	6.6.12
$\varepsilon_{th,m}$ (kWh/kg)	specific thermal energy consumption per unit mass of hydrogen under SATP conditions	6.6.12
$\eta_{HHV,e}^0$ (%)	energy efficiency based on HHV under SATP conditions of hydrogen	6.6.13
$\eta_{LHV,e}^0$ (%)	energy efficiency based on LHV under SATP conditions of hydrogen	6.6.13
$\eta_{HHV,el}^0$ (%)	electrical efficiency based on HHV under SATP conditions of hydrogen	6.6.13
$\eta_{LHV,el}^0$ (%)	electrical efficiency based on LHV under SATP conditions of hydrogen	6.6.13
SC (%)	steam conversion	6.6.13
η_F (%)	Faradaic efficiency	6.6.13

Note: According to the test plan (section 6.5), TOPs may be obtained as functions of TIPs or other TOPs as well as time (test duration), number of operation profiles (duty cycles) or sequence(s) of operation profiles (duty cycles). By adding appropriate indices to the symbol of the concerned TOP, TOPs of same type can be distinguished.

⁽¹⁾ conveyed by heat transfer fluids such as air and steam

⁽²⁾ conveyed by compressible fluids such as air and steam

⁽³⁾ in relation to input power, input current or input voltage, see section 6.6.5

⁽⁴⁾ for positive and negative ramps

⁽⁵⁾ from FC mode to electrolysis mode and from electrolysis mode to FC mode

⁽⁶⁾ hydrogen output rate, see equation (6.6.1)

⁽⁷⁾ oxygen output rate

⁽⁸⁾ When the polarisation curve measurement is conducted under potentiostatic conditions or by a set voltage ramp rate (\dot{U}).

⁽⁹⁾ When the polarisation curve measurement is conducted under galvanostatic conditions or by a set current ramp rate (\dot{I}).

⁽¹⁰⁾ When small amplitude AC voltage perturbations are used in EIS measurements.

⁽¹¹⁾ When small amplitude AC perturbations are used in EIS measurements.

Source: JRC, 2023

Table 7.2: Test results of durability tests

Symbol (unit)	Description	Test method
<i>Constant stack operation</i> ⁽¹⁾		
$\Delta_{\text{tot}}^k U$ ($\mu\text{V}/\text{h}$)	total rate of change of voltage ⁽²⁾	6.8.2
$\Delta_{\text{rel}}^k U$ ($\mu\text{V}/\text{h}$)	relative rate of change of voltage ⁽²⁾	6.8.2
$\Delta_{\text{tot}}^k R_{\text{ASR}}$ ($\text{m}\Omega \text{ cm}^2/\text{h}$)	total rate of change of area-specific resistance	6.8.2
$\Delta_{\text{rel}}^k R_{\text{ASR}}$ ($\text{m}\Omega \text{ cm}^2/\text{h}$)	relative rate of change of area-specific resistance	6.8.2
$\Delta_{\text{tot}}^k \eta_{\text{F}}$ ($\%/ \text{h}$)	total rate of change of Faradaic efficiency	6.8.2
$\Delta_{\text{rel}}^k \eta_{\text{F}}$ ($\%$)	relative rate of change of Faradaic efficiency	6.8.2
<i>Variable stack operation</i> ⁽¹⁾		
$\Delta_{\text{tot}}^k U$ ($\mu\text{V}/\text{h}$)	total rate of change of voltage ⁽²⁾	6.8.3
$\Delta_{\text{rel}}^k U$ ($\mu\text{V}/\text{h}$)	relative rate of change of voltage ⁽²⁾	6.8.3
$\Delta_{\text{tot}}^k R_{\text{ASR}}$ ($\text{m}\Omega \text{ cm}^2/\text{h}$)	total rate of change of area-specific resistance	6.8.3
$\Delta_{\text{rel}}^k R_{\text{ASR}}$ ($\text{m}\Omega \text{ cm}^2/\text{h}$)	relative rate of change of area-specific resistance	6.8.3
$\Delta_{\text{tot}}^k \eta_{\text{F}}$ ($\%/ \text{h}$)	total rate of change of Faradaic efficiency	6.8.3
$\Delta_{\text{rel}}^k \eta_{\text{F}}$ ($\%$)	relative rate of change of Faradaic efficiency	6.8.3
<i>Constant system operation</i> ⁽¹⁾		
$\Delta_{\text{tot}}^k \varepsilon_{\text{e,v}}$ ($(\text{J}/\text{m}^3)/\text{h}$)	total rate of change of specific energy consumption per unit volume of hydrogen under SATP conditions	6.8.2
$\Delta_{\text{rel}}^k \varepsilon_{\text{e,v}}$ ($(\text{J}/\text{m}^3)/\text{h}$)	relative rate of change of specific energy consumption per unit volume of hydrogen under SATP conditions	6.8.2
$\Delta_{\text{tot}}^k \varepsilon_{\text{e,m}}$ ($(\text{J}/\text{kg})/\text{h}$)	total rate of change of specific energy consumption per unit mass of hydrogen under SATP conditions	6.8.2
$\Delta_{\text{rel}}^k \varepsilon_{\text{e,m}}$ ($(\text{J}/\text{kg})/\text{h}$)	relative rate of change of specific energy consumption per unit mass of hydrogen under SATP conditions	6.8.2
$\Delta_{\text{tot}}^k \varepsilon_{\text{el,v}}$ ($(\text{J}/\text{m}^3)/\text{h}$)	total rate of change of specific electric energy consumption per unit volume of hydrogen under SATP conditions	6.8.2
$\Delta_{\text{rel}}^k \varepsilon_{\text{el,v}}$ ($(\text{J}/\text{m}^3)/\text{h}$)	relative rate of change of specific electric energy consumption per unit volume of hydrogen under SATP conditions	6.8.2
$\Delta_{\text{tot}}^k \varepsilon_{\text{el,m}}$ ($(\text{J}/\text{kg})/\text{h}$)	total rate of change of specific electric energy consumption per unit mass of hydrogen under SATP conditions	6.8.2
$\Delta_{\text{rel}}^k \varepsilon_{\text{el,m}}$ ($(\text{J}/\text{kg})/\text{h}$)	relative rate of change of specific electric energy consumption per unit mass of hydrogen under SATP conditions	6.8.2
$\Delta_{\text{tot}}^k \varepsilon_{\text{th,v}}$ ($(\text{J}/\text{m}^3)/\text{h}$)	total rate of change of specific thermal energy consumption per unit volume of hydrogen under SATP conditions	6.8.2
$\Delta_{\text{rel}}^k \varepsilon_{\text{th,v}}$ ($(\text{J}/\text{m}^3)/\text{h}$)	relative rate of change of specific thermal energy consumption per unit volume of hydrogen under SATP conditions	6.8.2
$\Delta_{\text{tot}}^k \varepsilon_{\text{th,m}}$ ($(\text{J}/\text{kg})/\text{h}$)	total rate of change of specific thermal energy consumption per unit mass of hydrogen under SATP conditions	6.8.2
$\Delta_{\text{rel}}^k \varepsilon_{\text{th,m}}$ ($(\text{J}/\text{kg})/\text{h}$)	relative rate of change of specific thermal energy consumption per unit mass of hydrogen under SATP conditions	6.8.2
$\Delta_{\text{tot}}^k \eta_{\text{HHV,e}}^0$ ($\%/ \text{h}$)	total rate of change of energy efficiency based on HHV under SATP conditions of hydrogen	6.8.2
$\Delta_{\text{rel}}^k \eta_{\text{HHV,e}}^0$ ($\%$)	relative rate of change of energy efficiency based on HHV under SATP conditions of hydrogen	6.8.2
$\Delta_{\text{tot}}^k \eta_{\text{LHV,e}}^0$ ($\%/ \text{h}$)	total rate of change of energy efficiency based on LHV under SATP conditions of hydrogen	6.8.2
$\Delta_{\text{rel}}^k \eta_{\text{LHV,e}}^0$ ($\%$)	relative rate of change of energy efficiency based on LHV under SATP conditions of hydrogen	6.8.2

Continue to next page

Table 7.2 – continued from previous page

$\Delta_{\text{tot}}^k \eta_{\text{HHV,el}}^0$ (%/h)	total rate of change of electrical efficiency based on HHV under SATP conditions of hydrogen	6.8.2
$\Delta_{\text{rel}}^k \eta_{\text{HHV,el}}^0$ (%)	relative rate of change of electrical efficiency based on HHV under SATP conditions of hydrogen	6.8.2
$\Delta_{\text{tot}}^k \eta_{\text{LHV,el}}^0$ (%/h)	total rate of change of electrical efficiency based on LHV under SATP conditions of hydrogen	6.8.2
$\Delta_{\text{rel}}^k \eta_{\text{LHV,el}}^0$ (%)	relative rate of change of electrical efficiency based on LHV under SATP conditions of hydrogen	6.8.2
<i>Variable system operation</i> ⁽¹⁾		
$\Delta_{\text{tot}}^k \varepsilon_{e,v}$ ((J/m ³)/h)	total rate of change of specific energy consumption per unit volume of hydrogen under SATP conditions	6.8.3
$\Delta_{\text{rel}}^k \varepsilon_{e,v}$ ((J/m ³)/h)	relative rate of change of specific energy consumption per unit volume of hydrogen under SATP conditions	6.8.3
$\Delta_{\text{tot}}^k \varepsilon_{e,m}$ ((J/kg)/h)	total rate of change of specific energy consumption per unit mass of hydrogen under SATP conditions	6.8.3
$\Delta_{\text{rel}}^k \varepsilon_{e,m}$ ((J/kg)/h)	relative rate of change of specific energy consumption per unit mass of hydrogen under SATP conditions	6.8.3
$\Delta_{\text{tot}}^k \varepsilon_{el,v}$ ((J/m ³)/h)	total rate of change of specific electric energy consumption per unit volume of hydrogen under SATP conditions	6.8.3
$\Delta_{\text{tot}}^k \varepsilon_{el,m}$ ((J/kg)/h)	total rate of change of specific electric energy consumption per unit mass of hydrogen under SATP conditions	6.8.3
$\Delta_{\text{rel}}^k \varepsilon_{el,m}$ ((J/kg)/h)	relative rate of change of specific electric energy consumption per unit mass of hydrogen under SATP conditions	6.8.3
$\Delta_{\text{tot}}^k \varepsilon_{th,v}$ ((J/m ³)/h)	total rate of change of specific thermal energy consumption per unit volume of hydrogen under SATP conditions	6.8.3
$\Delta_{\text{rel}}^k \varepsilon_{th,v}$ ((J/m ³)/h)	relative rate of change of specific thermal energy consumption per unit volume of hydrogen under SATP conditions	6.8.3
$\Delta_{\text{tot}}^k \varepsilon_{th,m}$ ((J/kg)/h)	total rate of change of specific thermal energy consumption per unit mass of hydrogen under SATP conditions	6.8.3
$\Delta_{\text{rel}}^k \varepsilon_{th,m}$ ((J/kg)/h)	relative rate of change of specific thermal energy consumption per unit mass of hydrogen under SATP conditions	6.8.3
$\Delta_{\text{tot}}^k \eta_{\text{HHV,e}}^0$ (%/h)	total rate of change of energy efficiency based on HHV under SATP conditions of hydrogen	6.8.3
$\Delta_{\text{rel}}^k \eta_{\text{HHV,e}}^0$ (%)	relative rate of change of energy efficiency based on HHV under SATP conditions of hydrogen	6.8.3
$\Delta_{\text{tot}}^k \eta_{\text{LHV,e}}^0$ (%/h)	total rate of change of energy efficiency based on LHV under SATP conditions of hydrogen	6.8.3
$\Delta_{\text{rel}}^k \eta_{\text{LHV,e}}^0$ (%)	relative rate of change of energy efficiency based on LHV under SATP conditions of hydrogen	6.8.3
$\Delta_{\text{tot}}^k \eta_{\text{HHV,el}}^0$ (%/h)	total rate of change of electrical efficiency based on HHV under SATP conditions of hydrogen	6.8.3
$\Delta_{\text{rel}}^k \eta_{\text{HHV,el}}^0$ (%)	relative rate of change of electrical efficiency based on HHV under SATP conditions of hydrogen	6.8.3
$\Delta_{\text{tot}}^k \eta_{\text{LHV,el}}^0$ (%/h)	total rate of change of electrical efficiency based on LHV under SATP conditions of hydrogen	6.8.3
$\Delta_{\text{rel}}^k \eta_{\text{LHV,el}}^0$ (%)	relative rate of change of electrical efficiency based on LHV under SATP conditions of hydrogen	6.8.3

Note: According to the test plan (section 6.5), TOPs may be obtained as functions of TIPs or other TOPs as well as time (test duration), number of operation profiles (duty cycles) or sequence(s) of operation profiles (duty cycles). By adding appropriate indices to the symbol of the concerned TOP, TOPs of same type can be distinguished.

⁽¹⁾ The test results are meant for each interval k.

⁽²⁾ In the absence of polarisation curve measurements (see footnote 41), the stack voltage may be replaced by the temperature of the stack operated under quasi-potentiostatic conditions (section 6.2); see also footnote 42.

Source: JRC, 2023

The test results should, as appropriate, be reported along with their standard uncertainties (*u*) in accordance with GUM (JCGM, 2008, JCGM, 2009, JCGM, 2020).

In addition to tabulated test results, TOPs may also be presented graphically (Annex C), for example, showing their evolution with time or the number and sequence(s) of operation profiles (duty cycles) as well as

presenting them as functions of TIPs (power, current, voltage, etc). Standard uncertainties of base quantities (current, voltage, flow rate, pressure, temperature, etc) and combined standard uncertainties (u_c) of derived quantities (power, specific energy consumption, efficiency, etc) may be displayed as error bars for a specified level of confidence.

8 Conclusions with final remarks

This report provides testing protocols for establishing the performance and durability of HTE stacks and HTSEL systems generating hydrogen in P2H2 applications for HtP, hydrogen-to-mobility (HtM) and H2I processes. They rely on test methods of ISO and IEC standards as well as on testing procedures previously developed in FCH2JU funded projects and those published as part of the EU electrolysis harmonisation activities.

These protocols allow for an adequate comparison of HTE technologies in stacks whether of SOEC type in SOE including rSOE, or PCEC type in PCE including rPCE. They also allow to compare the performance and durability of different HTSEL systems. Intended for use by the research community and industry alike, these protocols provide for built-in flexibility as performance tests may selectively be executed and application-oriented duty cycles may be added to the exemplified operation profiles.

Also, the user is free to add other performance tests for a particular test campaign as well as to substitute one or another test method or testing procedure when deemed more appropriate for the intended use of the stack or system in the application concerned. This is provided all tests are conducted safely (Annex A) and with due care, the recording of all relevant test parameters whether TIPs or TOPs is followed as required and the test results including uncertainties and measurement set-up(s) are adequately reported.

The performance and durability tests may be used to conduct accelerated stress testing (AST) (4.1.2) of a test item when degradation mechanisms and their triggering test conditions are known to affect the test item the same way as long exposures under normal conditions of use would do. This is a current subject of ongoing HTE research. Durability tests may be used to conduct accelerated lifetime testing (ALT) (4.1.1) of a test item for determining the item's RUL when aggravated conditions of use have previously been identified. This is yet to become a subject of electrolyser R&D.

References

- de Marco, G., Kotsionopoulos, N., Malkow, T., Couturier, K. and Lang, M., 'Current-voltage Characteristics', SOCT-ESQA Test Module 03, Joint Research Centre, Deutsches Zentrum für Luft- und Raumfahrt e.V., Commissariat à l'énergie atomique et aux énergies alternatives, 2017. URL <https://elib.dlr.de/119895/2/tm03b-jv.pdf>.
- CEA, 'Reversible solid oxide Electrolyzer and Fuel cell for optimized Local Energy mix', Project information, CORDIS, 2018. doi:10.3030/779577. URL <https://cordis.europa.eu/project/id/779577>.
- CEA, 'Multimegawatt high-temperature electrolyser to generate green hydrogen for production of high-quality biofuels', Project information, CORDIS, 2020. doi:10.3030/875123. URL <https://cordis.europa.eu/project/id/875123>.
- DLR, 'Solid Oxide Cell and Stack Testing, Safety and Quality Assurance', Project information, CORDIS, 2014. URL <https://cordis.europa.eu/project/id/621245>.
- JCGM, 'Evaluation of measurement data - Guide to the expression of uncertainty in measurement', GUM: Guide to the Expression of Uncertainty in Measurement JCGM 100:2008, Joint Committee for Guides in Metrology, 2008. URL https://www.bipm.org/utils/common/documents/jcgm/JCGM_100_2008_E.pdf.
- JCGM, 'Evaluation of measurement data - An introduction to the Guide to the expression of uncertainty in measurement and related documents', GUM: Guide to the Expression of Uncertainty in Measurement JCGM 104:2009, Joint Committee for Guides in Metrology, 2009. URL https://www.bipm.org/documents/20126/2071204/JCGM_104_2009.pdf.
- JCGM, 'Guide to the expression of uncertainty in measurement - Part 6: Developing and using measurement models', GUM: Guide to the Expression of Uncertainty in Measurement JCGM GUM-6:2020, Joint Committee for Guides in Metrology, 2020. URL https://www.bipm.org/documents/20126/2071204/JCGM_GUM_6_2020.pdf/d4e77d99-3870-0908-ff37-c1b6a230a337?version=1.8&t=1659083073972&download=true.
- SINTEF, 'Game changer in high temperature steam electrolyzers with novel tubular cells and stacks geometry for pressurized hydrogen production', Project information, CORDIS, 2018. doi:10.3030/779486. URL <https://cordis.europa.eu/project/id/779486>.
- Kröger, F. A. and Vink, H. J., 'Relations between the Concentrations of Imperfections in Crystalline Solids', *Solid State Physics*, Vol. 3, No C, 1956, pp. 307–435. doi:10.1016/S0081-1947(08)60135-6.
- Kröger, F. A. and Vink, H. J., 'Relations between the concentrations of imperfections in solids', *Journal of Physics and Chemistry of Solids*, Vol. 5, No 3, 1958, pp. 208–223. doi:10.1016/0022-3697(58)90069-6.
- Shih, A. J., de Oliveira Monteiro, M. C., Dattila, F., Pavesi, D., Philips, M., Marques da Silva, A. H., Vos, R. E., Ojha, K., Park, S., van der Heijden, O., Marcandalli, G., Goyal, A., Villalba, M., Chen, X., Gunasooriya, G. T. K. K., McCrum, I., Mom, R., López, N. and Koper, M. T. M., 'Water electrolysis', *Nature Reviews Methods Primers*, Vol. 2, 2022, p. 84. doi:10.1038/s43586-022-00164-0.
- McPhail, S. J., Frangini, S., Laurencin, J., Effori, E., Abaza, A., Padinjarethil, A. K., Hagen, A., Léon, A., Brisse, A., Vladikova, D., Burdin, B., Bianchi, F. R., Bosio, B., Piccardo, P., Spotorno, R., Uchida, H., Polverino, P., Adinolfi, E. A., Postiglione, F., Lee, J.-H., Moussaoui, H. and Van herle, J., 'Addressing planar solid oxide cell degradation mechanisms: A critical review of selected components', *Electrochemical Science Advances*, Vol. 2, No 5, 2022, p. e2100024. doi:10.1002/elsa.202100024.
- Mushtaq, U., Welzel, S., Sharma, R. K., van de Sanden, M. C. M. and Tsampas, M. N., 'Development of electrode-supported proton conducting solid oxide cells and their evaluation as electrochemical hydrogen pumps', *ACS Applied Materials & Interfaces*, Vol. 14, No 34, 2022, pp. 38938–38951. doi:10.1021/acsami.2c11779.
- Bianchi, F. R. and Bosio, B., 'Operating principles, performance and technology readiness level of reversible solid oxide cells', *Sustainability*, Vol. 13, 2021, p. 4777. doi:10.3390/su13094777.
- Lang, M., Wenz, F., Braniek, G., Auer, C., Sun, X., Høgh, J., Fu, Q., Liu, Q. and Couturier, K., 'Electrochemical Impedance Spectroscopy', SOCTESQA Test Module 04, Deutsches Zentrum für Luft- und Raumfahrt e.V., Danmarks Tekniske Universitet, Europäisches Institut für Energieforschung, Nanyang Technological University Singapore, Commissariat à l'énergie atomique et aux énergies alternatives, 2017. URL <https://elib.dlr.de/119896/1/tm04b-eis.pdf>.

EP and Council, 'Approximation of the laws of the Member States concerning equipment and protective systems intended for use in potentially explosive atmospheres', Directive 94/9/EC, Publications Office of the European Union, Brussels (BE), 23 March 1994. URL <http://data.europa.eu/eli/dir/1994/9/oj>. OJ L 100 of 19.4.1994.

EP and Council, 'General Product Safety', Directive 2001/95/EC, Publications Office of the European Union, Brussels (BE), 3 December 2001. URL <http://data.europa.eu/eli/dir/2001/95/oj>. OJ L 11 of 15.1.2002.

EP and Council, 'Machinery, and amending Directive 95/16/EC', Directive 2006/42/EC, Publications Office of the European Union, Brussels (BE), 17 May 2006. URL <http://data.europa.eu/eli/dir/2006/42/oj>. OJ L 157 of 9.6.2006.

EP and Council, 'Harmonisation of the laws of the Member States relating to electromagnetic compatibility', Directive 2014/30/EU, Publications Office of the European Union, Brussels (BE), 26 February 2014a. URL <http://data.europa.eu/eli/dir/2014/30/oj>. OJ L 96 of 29.3.2014.

EP and Council, 'Harmonisation of the laws of the Member States relating to equipment and protective systems intended for use in potentially explosive atmospheres', Directive 2014/34/EU, Publications Office of the European Union, Brussels (BE), 26 February 2014b. URL <http://data.europa.eu/eli/dir/2014/34/oj>. OJ L 96 of 29.3.2014.

EP and Council, 'Harmonisation of the laws of the Member States relating to the making available on the market of electrical equipment designed for use within certain voltage limits', Directive 2014/35/EU, Publications Office of the European Union, Brussels (BE), 26 February 2014c. URL <http://data.europa.eu/eli/dir/2014/35/oj>. OJ L 96 of 29.3.2014.

EP and Council, 'Harmonisation of the laws of the Member States relating to the making available on the market of pressure equipment', Directive 2014/68/EU, Publications Office of the European Union, Brussels (BE), 15 May 2014d. URL <http://data.europa.eu/eli/dir/2014/68/oj>. OJ L 189 of 27.6.2014.

IEC, 'Explosive atmospheres - Part 17: Electrical installations inspection and maintenance', International Standard IEC 60079-17:2013, International Electrotechnical Commission, Geneva (CH), 2013. URL <https://webstore.iec.ch/publication/631>.

IEC, 'Explosive atmospheres - Part 14: Electrical installations design, selection and erection', International Standard IEC 60079-14:2013, International Electrotechnical Commission, Geneva (CH), 2014a. URL <https://webstore.iec.ch/publication/628>.

IEC, 'Fuel cell technologies - Part 7-2: Test methods - Single cell and stack performance tests for solid oxide fuel cells (SOFC)', International Standard IEC 62282-7-2:2014, International Electrotechnical Commission, Geneva (CH), 2014b. URL <https://webstore.iec.ch/publication/6766>.

IEC, 'Safety requirements for electrical equipment for measurement, control, and laboratory use - Part 1: General requirements', International Standard IEC 61010-1:2010+AMD1:2016 CSV, International Electrotechnical Commission, Geneva (CH), 2016. URL <https://webstore.iec.ch/publication/59769>.

IEC, 'Explosive atmospheres - Part 0: Equipment - General requirements', International Standard IEC 60079-0:2017, International Electrotechnical Commission, Geneva (CH), 2017. URL <https://webstore.iec.ch/publication/32878>.

IEC, 'Fuel cell technologies - Part 3-100: Stationary fuel cell power systems - Safety', International Standard IEC 62282-3-100:2019, International Electrotechnical Commission, Geneva (CH), 2019. URL <https://webstore.iec.ch/publication/59780>.

IEC, 'Explosive atmospheres - Part 10-1: Classification of areas - Explosive gas atmospheres', International Standard IEC 60079-10-1:2020, International Electrotechnical Commission, Geneva (CH), 2020a. URL <https://webstore.iec.ch/publication/63327>.

IEC, 'Fuel cell technologies - Part 2-100: Fuel cell modules - Safety', International Standard IEC 62282-2-100:2020, International Electrotechnical Commission, Geneva (CH), 2020b. URL <https://webstore.iec.ch/publication/59780>.

IEC, 'Fuel cell technologies - Part 8-101: Energy storage systems using fuel cell modules in reverse mode - Test procedures for the performance of solid oxide single cells and stacks, including reversible operation', International Standard IEC 62282-8-101:2020, International Electrotechnical Commission, Geneva (CH), 2020c. URL <https://webstore.iec.ch/publication/33278>.

IEC, 'Fuel cell technologies - Part 8-201: Energy storage systems using fuel cell modules in reverse mode - Test procedures for the performance of power-to-power systems', International Standard IEC 62282-8-201:2020, International Electrotechnical Commission, Geneva (CH), 2020d. URL <https://webstore.iec.ch/publication/31519>.

IEC, 'Safety of machinery - Electrical equipment of machines - Part 1: General requirements', International Standard IEC 60204-1:2016+AMD1:2021 CSV, International Electrotechnical Commission, Geneva (CH), 2021. URL <https://webstore.iec.ch/publication/71256>.

IEC, 'Amendment 1 - Fuel cell technologies - Part 3-201: Stationary fuel cell power systems - Performance test methods for small fuel cell power systems', International Standard IEC 62282-3-201:2017+AMD1:2022 CSV, International Electrotechnical Commission, Geneva (CH), 2022. URL <https://webstore.iec.ch/publication/65282>.

IEEE, 'Standard Definitions for the Measurement of Electric Power Quantities Under Sinusoidal, Nonsinusoidal, Balanced, or Unbalanced Conditions', Standard IEEE 1459:2010 (Revision of IEEE Std 1459-2000) - Redline, Institute of Electrical and Electronics Engineers, New York (NY), 2010. doi:10.1109/IEEESTD.2010.5953405. URL <https://ieeexplore.ieee.org/servlet/opac?punumber=5953403>.

ISO, 'Hydrogen generators using fuel processing technologies - Part 2: Test method for performance', International Standard ISO 16110-2:2010, International Organization for Standardization, Geneva (CH), 2010. URL <https://www.iso.org/standard/41046.html>.

ISO, 'Basic considerations for the safety of hydrogen systems', Technical Report ISO/TR 15916:2015, International Organization for Standardization, Geneva (CH), 2015. URL <https://www.iso.org/standard/69212.html>.

ISO, 'Occupational health and safety management systems - Requirements with guidance for use', International Standard ISO 45001:2018, International Organization for Standardization, Geneva (CH), 2018. URL <https://www.iso.org/standard/63787.html>.

ISO, 'Hydrogen generators using water electrolysis - Industrial, commercial, and residential applications', International Standard ISO 22734:2019, International Organization for Standardization, Geneva (CH), 2019. URL <https://www.iso.org/standard/69212.html>.

ISO and IEC, 'Principles and rules for the structure and drafting of ISO and IEC documents', ISO/IEC Directives, Part 2, Ninth edition, International Organization for Standardization, International Electrotechnical Commission, Geneva (CH), 2021. URL <https://www.iso.org/sites/directives/current/part2/index.xhtml>.

Kee, B. L., Curran, D., Zhu, H., Braun, R. J., DeCaluwe, S. C., Kee, R. J. and Ricote, S., 'Thermodynamic insights for electrochemical hydrogen compression with proton-conducting membranes', *membranes*, Vol. 9, No 7, 2019, p. 77. doi:10.3390/membranes9070077.

Duan, C., Huang, J., Sullivan, N., and O'Hayre, R., 'Proton-conducting oxides for energy conversion and storage', *Applied Physics Review*, Vol. 7, 2020, p. 011314. doi:10.1063/1.5135319.

Graves, C., Hauch, A., Pylypko, S., Di Iorio, S., Petitjean, M. and Cubizolles, G., 'Cells and Stacks testing protocol', REFLEX Deliverable D 2.1, Commissariat à l'énergie atomique et aux énergies alternatives, Danmarks Tekniske Universitet, Elcogen AS, 2018. URL <https://www.reflex-energy.eu/-/media/sites/reflex/deliverables/deliverables-updatet-with-eu-logo/d2-1-cells-and-stacks-testing-protocol-public-version.pdf>.

Vøllestad, E., Norby, T., Marie-Laure Fontaine, Michael Budd, Vestre, P. K., Tarach, M. and Serra, J. M., 'Definition of protocols and criteria for qualification testing', GAMER Deliverable D 3.1, Universitetet i Oslo, Stiftelsen for industriell og teknisk forskning, CoorsTek Membrane Sciences AS, Consejo Superior de Investigaciones Científicas - Instituto de Tecnología Química, 2018. URL <https://www.sintef.no/globalassets/project/gamer/deliverable-d3.1-28-02-2018-final.pdf>.

Tsotridis, G. and Pilenga, A., 'EU harmonised terminology for low temperature water electrolysis for energy storage applications', JRC112082, EUR 29300 EN, KJ-NA-29300-EN-N (online), KJ-NA-29300-EN-C (print). Publications Office of the European Union, Luxembourg (L), 2018. ISBN 978-92-79-90387-8 (online), 978-92-79-90388-5 (print). doi:10.2760/138987(online),10.2760/014448(print). URL <http://publications.jrc.ec.europa.eu/repository/handle/JRC112082>.

- Tsotridis, G. and Pilenga, A., 'EU harmonised protocols for testing of low temperature water electrolyzers', JRC122565, EUR 30752 EN, KJ-NA-30752-EN-N (online), KJ-NA-30752-EN-C (print). Publications Office of the European Union, Luxembourg (L), 2021. ISBN 978-92-76-39266-8 (online), 978-92-76-39265-1 (print). doi:10.2760/58880(online),10.2760/502481(print). URL <https://publications.jrc.ec.europa.eu/repository/handle/JRC122565>.
- Sdanghi, G., Maranzana, G., Celzard, A. and Fierro, V., 'Towards non-mechanical hybrid hydrogen compression for decentralized hydrogen facilities', *energies*, Vol. 13, 2020, p. 3145. doi:10.3390/en13123145.
- Aicart, J., Surrey, A. and Nechache, A., 'Definition of Testing Protocols', MultiPLHY Deliverable D 2.1, Commissariat à l'énergie atomique et aux énergies alternatives, Sunfire GmbH, Engie SA, 2020. URL <https://cordis.europa.eu/project/id/875123/results>.
- Chatenet, M., Pollet, B. G., Dekel, D. R., Dionigi, F., Deseure, J., Millet, P., Braatz, R. D., Bazant, M. Z., Eikerling, M., Staffell, I., Balcombe, P., Shao-Horn, Y. and Schäfer, H., 'Water electrolysis: from textbook knowledge to the latest scientific strategies and industrial developments', *Chemical Society Reviews*, Vol. 51, 2022, pp. 4583–4762. doi:10.1039/DOCS01079K.
- Tahan, M.-R., 'Recent advances in hydrogen compressors for use in large-scale renewable energy integration', *International Journal of Hydrogen Energy*, Vol. 47, No 83, 2022, pp. 35275–35292. doi:10.1016/j.ijhydene.2022.08.128.
- Ebbesen, S. D., Jensen, S. H., Hauch, A. and Mogensen, M. B., 'High temperature electrolysis in alkaline cells, solid proton conducting cells, and solid oxide cells', *Chemical Reviews*, Vol. 114, No 21, 2014, pp. 10697–10734. doi:10.1021/cr5000865.
- Durmuş, G. N. B., Özgür Çolpan, C. and Devrim, Y., 'A review on the development of the electrochemical hydrogen compressors', *Journal of Power Sources*, Vol. 494, 2021, p. 229743. doi:10.1016/j.jpowsour.2021.229743.
- Lang, M., Bohn, C., Couturier, K., Sun, X., McPhail, S. J., Malkow, T., Pilenga, A., Fu, Q. and Liu, Q., 'Electrochemical Quality Assurance of Solid Oxide Electrolyser (SOEC) Stacks', *Journal of The Electrochemical Society*, Vol. 166, No 15, 2019, pp. F1180–F1189. doi:10.1149/2.0041915jes.
- Malkow, K. T., Pilenga, A. and Blagoeva, D., 'EU harmonised terminology for hydrogen generated by electrolysis', EUR 30324 EN, KJ-NA-30324-EN-N (online), KJ-NA-30324-EN-C (print). Publications Office of the European Union, Luxembourg (L), 2021. ISBN 978-92-76-21042-9 (online), 978-92-76-21041-2 (print). doi:10.2760/293538(print),10.2760/732809(online). URL <https://publications.jrc.ec.europa.eu/repository/handle/JRC120120>.
- Malkow, T. and Pilenga, A., 'EU harmonised testing procedure: Determination of water electrolyser energy performance', Validated Methods, Reference Methods and Measurements Report KJ-07-22-323-EN-N, Publications Office of the European Union, Luxembourg (L), 2023. doi:10.2760/922894. URL <https://publications.jrc.ec.europa.eu/repository/handle/JRC128292>.
- Malkow, T., Lang, M. and Auer, C., 'List of SOC test procedures', SOCTESQA Deliverable Report D.2.2, Joint Research Centre, Deutsches Zentrum für Luft- und Raumfahrt e. V., 2014. URL https://elib.dlr.de/121084/1/D2_2_List_SOC_Test_Procedures_submit.pdf.
- Marcuš, D., Kovač, A. and Firak, M., 'Electrochemical hydrogen compressor: Recent progress and challenges', *International Journal of Hydrogen Energy*, Vol. 47, No 57, 2022, pp. 24179–24193. doi:10.1016/j.ijhydene.2022.04.134.
- Zou, J., Han, N., Yan, J., Feng, Q., Wang, Y., Zhao, Z., Fan, J., Zeng, L., Li, H. and Wang, H., 'Electrochemical compression technologies for high-pressure hydrogen: Current status, challenges and perspective', *Electrochemical Energy Reviews*, Vol. 3, 2020, p. 690–729. doi:10.1007/s41918-020-00077-0.

List of Abbreviations and Acronyms

AC	alternating current
AC/DC	alternating current-to-direct current
AEL	alkaline water electrolysis
ALT	accelerated lifetime testing
AMD	amendment
AS	Aktsiaselts
ASR	area-specific resistance
AST	accelerated stress testing
ATEX	Appareils destinés à être utilisés en atmosphères explosibles
AWE	alkaline water electrolyser
AWI	approved working item
BoL	beginning-of-life
BoP	balance of plant
BoT	beginning-of-test
BV	besloten vennootschap
CC BY 4.0	Creative Commons Attribution 4.0 International
CEA	Commissariat à l'énergie atomique et aux énergies alternatives
CGO	ceria-doped gadolinium oxide
CH	Switzerland
CH₂	compressed hydrogen
Clean H₂ JU	Clean Hydrogen Joint Undertaking
CMS	CoorsTek Membrane Sciences AS
CORDIS	Community Research and Development Information Service
CRI	Carbon Recycling International EHF
CSC	cathode-supported cell
CSIC	Consejo Superior de Investigaciones Científicas
CSV	consolidated version
DAQ	data acquisition
DC	direct current
DC/DC	direct current-to-direct current
DLR	Deutsches Zentrum für Luft- und Raumfahrt e. V.
doi	digital object identifier
DTU	Danmarks Tekniske Universitet
e. V.	eingetragener Verein
EC	European Commission
EEA	European Economic Area
EHC	electrochemical hydrogen compressor
EHF	einkahlutafélag
EIFER	Europäisches Institut für Energieforschung
EIS	electrochemical impedance spectroscopy
EMC	electromagnetic compatibility
EN	English
ENEA	Agenzia Nazionale per le Nuove tecnologie, l'Energia e lo Sviluppo economico sostenibile
End-of-test	
ES	energy-storage
ESC	electrolyte-supported cell
EU	European Union
EUR	European Union Report
FC	fuel cell
FCH₂JU	Fuel Cells and Hydrogen second Joint Undertaking
GAMER	Game changer in high temperature steam electrolyzers with novel tubular cells and stacks geometry for pressurized hydrogen production
GmbH	Gesellschaft mit beschränkter Haftung
GUM	Guide to the expression of uncertainty in measurement
H-SOE	hydrogen ion (proton) conducting solid oxide electrolyser
H₂I	hydrogen-to-industry
HER	hydrogen evolution reaction
HHV	higher heating value
HOR	hydrogen oxidation reaction

HTE high-temperature electrolyser
HTEL high-temperature electrolysis
HtM hydrogen-to-mobility
HtP hydrogen-to-power
HTSEL high-temperature steam electrolysis
IEC International Electrotechnical Commission
IEEE Institute of Electrical and Electronics Engineers
IEV International Electrotechnical Vocabulary
ISBN international standard book number
ISO International Organization for Standardization
JCGM Joint Committee for Guides in Metrology
JRC Joint Research Centre
KPI key performance indicator
L Luxembourg
LH₂ liquefied hydrogen
LHV lower heating value
LSC strontium-doped lanthanum cobalt oxide
LSCF strontium-doped lanthanum cobalt iron oxide
LTWE low-temperature water electrolysis
LVD Low-Voltage Directive
MIEC mixed ionic and electronic conductor
MSC metal-supported cell
MultiPLHY Multimegawatt high-temperature electrolyser to generate green hydrogen for production of high-quality biofuels
NG natural gas
NV naamloze vennootschap
NY New York
O-SOE oxygen ion-conducting solid oxide electrolyser
OCV open circuit voltage
OER oxygen evolution reaction
OHS occupational health and safety
OJ Official Journal
ORR oxygen reduction reaction
Oy Osakeyhtiö
Oyj julkinen Osakeyhtiö
P2C power-to-chemical
P2F power-to-fuel
P2G power-to-gas
P2H₂ power-to-hydrogen
P2L power-to-liquid
P2M power-to-mobility
P2P power-to-power
P2X power-to-X
PCC proton-conducting ceramic
PCCEL proton-conducting ceramic steam electrolysis
PCE proton-conducting ceramic electrolyser
PCEC proton-conducting ceramic electrolysis cell
PCFC proton-conducting ceramic fuel cell
PDF portable document format
PED Pressure Equipment Directive
PEM proton exchange polymer membrane
PEMEL proton exchange polymer membrane water electrolysis
PEMWE proton exchange polymer membrane water electrolyser
PIPC Polska Izba Przemysłu Chemicznego
PoC point of connection
PV photovoltaic
R&D research and development
R&I research and innovation
REFLEX Reversible solid oxide Electrolyzer and Fuel cell for optimized Local Energy miX
RES renewable energy source
rFC reversible fuel cell

rms root-mean-square
rPCC reversible proton-conducting ceramic electrolysis cell
rPCE reversible proton-conducting ceramic electrolyser
rSOC reversible solid oxide electrolysis cell
rSOE reversible solid oxide electrolyser
RUL remaining useful life
S.L. Sociedad Limitada
SA Société anonyme
SATP standard ambient temperature and pressure
SI Système International d'Unités
SINTEF Stiftelsen for industriell og teknisk forskning
SOC solid oxide cell
SOCTESQA Solid Oxide Cell and Stack Testing, Safety and Quality Assurance
SOE solid oxide electrolyser
SOEC solid oxide electrolysis cell
SOEL solid oxide steam electrolysis
SOFC solid oxide fuel cell
SRIA strategic research and innovation agenda 2021-2027 of the Clean Hydrogen Partnership for Europe
TC Technical Committee
TIP test input parameter
TM Test Module
TMA technology monitoring and assessment
TNO Nederlandse Organisatie voor Toegepast Natuurwetenschappelijk Onderzoek
TOP test output parameter
TR Technical Report
TRL technology readiness level
UiO Universitetet i Oslo
URL uniform resource locator
UV ultraviolet
VTT Teknologian tutkimuskeskus VTT Oy
WG working group
YSZ yttria-stabilised zirconia

List of Symbols

Notation	Description
(ed)	subscript denoting electrode
(el)	subscript denoting electrolyte
(g)	subscript denoting gaseous phase
A_{act}	active electrode area
CO_2	carbon dioxide
c_p	specific heat capacity at constant pressure
c_p^i	specific heat capacity at constant pressure of fluid i
c_p^j	specific heat capacity at constant pressure of fluid j
c_V^j	specific heat capacity at constant volume of fluid j
$\Delta_{rel}^k \varepsilon_{el,m}$	relative rate of change of specific electric energy consumption per unit mass of hydrogen
$\Delta_{rel}^k \varepsilon_{el,V}$	relative rate of change of specific electric energy consumption per unit volume of hydrogen
$\Delta_{rel}^k \varepsilon_{e,m}$	relative rate of change of specific energy consumption per unit mass of hydrogen
$\Delta_{rel}^k \varepsilon_{e,V}$	relative rate of change of specific energy consumption per unit volume of hydrogen
$\Delta_{rel}^k \varepsilon_{th,m}$	relative rate of change of specific thermal energy consumption per unit mass of hydrogen
$\Delta_{rel}^k \varepsilon_{th,V}$	relative rate of change of specific thermal energy consumption per unit volume of hydrogen
$\Delta_{rel}^k \eta_{HHV,e}^0$	relative rate of change of energy efficiency based on HHV under SATP conditions of hydrogen
$\Delta_{rel}^k \eta_{HHV,el}^0$	relative rate of change of electrical efficiency based on HHV under SATP conditions of hydrogen
$\Delta_{rel}^k \eta_{LHV,e}^0$	relative rate of change of energy efficiency based on LHV under SATP conditions of hydrogen
$\Delta_{rel}^k \eta_{LHV,el}^0$	relative rate of change of electrical efficiency based on LHV under SATP conditions of hydrogen
$\Delta_{rel}^k \eta_F$	relative rate of change of Faradaic efficiency
$\Delta_{rel}^k R_{ASR}$	relative rate of change of area-specific resistance
$\Delta_{rel}^k U$	relative rate of change of voltage
$\Delta_{tot}^k \varepsilon_{el,m}$	total rate of change of specific electric energy consumption per unit mass of hydrogen
$\Delta_{tot}^k \varepsilon_{el,V}$	total rate of change of specific electric energy consumption per unit volume of hydrogen
$\Delta_{tot}^k \varepsilon_{e,m}$	total rate of change of specific energy consumption per unit mass of hydrogen
$\Delta_{tot}^k \varepsilon_{e,V}$	total rate of change of specific energy consumption per unit volume of hydrogen
$\Delta_{tot}^k \varepsilon_{th,m}$	total rate of change of specific thermal energy consumption per unit mass of hydrogen
$\Delta_{tot}^k \varepsilon_{th,V}$	total rate of change of specific thermal energy consumption per unit volume of hydrogen
$\Delta_{tot}^k \eta_{HHV,e}^0$	total rate of change of energy efficiency based on HHV under SATP conditions of hydrogen
$\Delta_{tot}^k \eta_{HHV,el}^0$	total rate of change of electrical efficiency based on HHV under SATP conditions of hydrogen
$\Delta_{tot}^k \eta_{LHV,e}^0$	total rate of change of energy efficiency based on LHV under SATP conditions of hydrogen
$\Delta_{tot}^k \eta_{LHV,el}^0$	total rate of change of electrical efficiency based on LHV under SATP conditions of hydrogen
$\Delta_{tot}^k \eta_F$	total rate of change of Faradaic efficiency
$\Delta_{tot}^k R_{ASR}$	total rate of change of area-specific resistance
$\Delta_{tot}^k U$	total rate of change of voltage
E	energy

Notation	Description
e'	electron (in Kröger-Vink notation)
e^-	electron
E_{compr}	pneumatic energy
E_{el}	electric energy
E_{off}	shut-down energy
E_{on}	start-up energy
ε_e	specific energy consumption
ε_{el}	specific electric energy consumption
$\varepsilon_{\text{el,m}}$	specific electric energy consumption per unit mass of hydrogen
$\varepsilon_{\text{el,V}}$	specific electric energy consumption per unit volume of hydrogen
$\varepsilon_{e,m}$	specific energy consumption per unit mass of hydrogen
$\varepsilon_{e,V}$	specific energy consumption per unit volume of hydrogen
ε_{th}	specific thermal energy consumption
$\varepsilon_{\text{th,m}}$	specific thermal energy consumption per unit mass of hydrogen
$\varepsilon_{\text{th,V}}$	specific thermal energy consumption per unit volume of hydrogen
E_{ramp}	ramp energy
U_{rev}	voltage under reversible (equilibrium) conditions
η	efficiency
η_e	energy efficiency
$\eta_{\text{HHV,e}}^0$	energy efficiency based on HHV under SATP conditions of hydrogen
η_{el}	electrical efficiency
$\eta_{\text{HHV,el}}^0$	electrical efficiency based on HHV under SATP conditions of hydrogen
$\eta_{\text{LHV,e}}^0$	energy efficiency based on LHV under SATP conditions of hydrogen
$\eta_{\text{LHV,el}}^0$	electrical efficiency based on LHV under SATP conditions of hydrogen
η_{F}	Faradaic efficiency
E_{th}	thermal energy
F	Faraday constant
f	perturbation frequency
f_{max}	maximum frequency
f_{min}	minimum frequency
γ^j	isentropic expansion factor of fluid j
H	hydrogen
H^+	proton
h^\cdot	electron hole
H_2	molecular hydrogen
H_2O	steam
HHV ^f	higher heating value of fuel
I	current
I_{ac}	alternating current
I_{dc}	direct current
\dot{I}	current ramp rate
I_{in}	input current
I_{nom}	nominal (rated) current
I_{stack}	stack current
J	current density
J_{dc}	DC density
J_{stack}	stack current density
M_M^\cdot	singly negatively charged metal ion lattice site
N_{cells}	number of cells
O	oxygen
O_2	molecular oxygen
O^{2-}	oxygen ion
OH_O^\cdot	hydroxide ion at singly positively charged oxygen lattice site
O_O^x	neutral oxygen ion lattice site
P	power
p	pressure
p^0	standard ambient pressure

Notation	Description
p^{pos}	pressure at the positrode
p^{neg}	pressure at the negatrode
P_{compr}	power of compression
$P_{\text{compr, in}}$	input power of compression
P_{el}	electric power
$P_{\text{el, 1p, ac}}$	single-phase alternating current (AC) power
$P_{\text{el, 3p, ac}}$	symmetrical three-phase AC power
$P_{\text{el, ac}}$	AC power
$P_{\text{el, ac, in}}$	input AC power
$P_{\text{el, d}}$	electric power density
$P_{\text{el, dc}}$	DC power
$P_{\text{el, dc, in}}$	input DC power
$P_{\text{el, d, stack}}$	stack electric power density
$P_{\text{el, in}}$	input electric power
$P_{\text{el, nom}}$	nominal (rated) electric power
$P_{\text{el, stack}}$	stack electric power
$\cos \varphi$	power factor
p^{H_2}	partial pressure of hydrogen
$p^{\text{H}_2\text{O}}$	pressure of hydrogen
$p^{\text{H}_2\text{O}}$	partial pressure of water vapour (steam)
P_{in}	input power
p^j	pressure of fluid j
p^{O_2}	partial pressure of oxygen
P_{stack}	stack power
P_{th}	thermal power
$P_{\text{th, in}}$	input thermal power
q	flow rate
q_{m}	mass flow rate
q_{m}^i	mass flow rate of fluid i
q_{n}	molar flow rate
q_{n}^{f}	molar flow rate of fuel
$q_{\text{n, H}_2}$	molar flow rate of hydrogen
q_{n}^j	molar flow rate of fluid j
$q_{\text{n, O}_2}$	molar flow rate of oxygen
$q_{\text{n, out}}$	product gas molar flow rate
$q_{\text{V, H}_2}$	volumetric flow rate of hydrogen
$q_{\text{V, H}_2\text{O}}$	volumetric flow rate of steam
R_0	zero-frequency resistance
R_{ASR}	area-specific resistance
R_{g}	universal gas constant
R_{∞}	high-frequency resistance
R_{lf}	low-frequency resistance
R_{Ω}	ohmic resistance
R_{pol}	polarisation resistance
SC	steam conversion
T	temperature
t	time
T^0	standard ambient temperature
t_0	time at BoT
\dot{T}_{cool}	cooling rate
T_{H_2}	temperature of hydrogen
\dot{T}_{heat}	heating rate
T^i	temperature of fluid i
t_{k}	time at interval k
t_{off}	shut-down time
t_{on}	start-up time
t_{resp}	response time
T_{stack}	stack temperature
t_{switch}	switch-over time

Notation	Description
U	voltage
u	standard uncertainty
U_{ac}	AC voltage
u_c	combined standard uncertainty
U_{dc}	DC voltage
\dot{U}	voltage ramp rate
U_{in}	input voltage
U_{nom}	nominal (rated) voltage
U_{stack}	stack voltage
U_{tn}	thermal-neutral voltage
V	volume
$V_O^{\cdot\cdot}$	doubly positively charged oxygen ion lattice vacancy
V_{AC}	AC voltage
V_m	molar volume
V_{m, H_2}	molar volume of hydrogen
x_{n, H_2}	molar concentration of hydrogen
x_{n, O_2}	molar concentration of oxygen
Y	electrical admittance
Z	electrical impedance
\bar{Z}	average compressibility factor
\bar{Z}^j	average compressibility factor of fluid j

List of Figures

- Figure 1.1.** Schematic of a HTSEL system 4
- Figure 5.1.** Schematic of the input and output streams of energy forms and substances of a HTE stack . . . 14
- Figure 5.2.** Schematic of the input and output streams of energy forms and substances of a HTSEL system 15
- Figure 6.1.** Operation profile for testing electrolyser reactivity 24
- Figure 6.2.** Operation profile for testing electrolyser high flexibility 24
- Figure 6.3.** Operation profile for testing electrolyser 100 % flexibility 25
- Figure 6.4.** Operation profile for testing electrolyser 200 % flexibility 25

List of Tables

- Table 6.1.** Recommended reference operating conditions for HTE stacks 18
- Table 7.1.** Test results of performance tests 31
- Table 7.2.** Test results of durability tests 32
- Table B.1.** Reactivity operation profile data 50
- Table B.2.** High flexibility operation profile data 53
- Table B.3.** 100 % flexibility operation profile data 55
- Table B.4.** 200 % flexibility operation profile data 57

Annex A Test safety

In HTE stacks and HTSEL systems, hazards arises especially from

- generated hydrogen and oxygen gases,
- use of steam and other fluids (combustible fuel, compressed air, hydraulic oil, etc) and
- high temperature, high pressure and high voltage.

During installation, commissioning, operation including quiescence and maintenance as well as decommissioning, the safety of persons requires due care and vigilance by all parties.

The entity carrying out the testing should comply with the occupational health and safety (OHS) requirements of ISO 45001:2018 (ISO, 2018).

Tests on HTE stacks and HTSEL systems shall be conducted in accordance with the applicable legislation, granted licenses and issued permits not to pose harm or unacceptable risk to humans, property and the environment.

ISO has published guidance regarding basic safety considerations for systems (ISO, 2015) ⁽⁵¹⁾ which shall be observed while testing HTE stacks and HTSEL systems ⁽⁵²⁾. Additionally, IEC published guidance on the classification of areas where explosive atmospheres occur (IEC, 2014a, IEC, 2013, IEC, 2017, IEC, 2020a) which shall also be followed.

Note, IEC published standards on FC safety (IEC, 2019, IEC, 2020b) which may be applied by analogy as appropriate ⁽⁵³⁾.

In the European Economic Area (EEA) ⁽⁵⁴⁾, the ATEX Directives 2014/34/EU (EP and Council, 2014b) and 94/9/EC (EP and Council, 1994) apply ⁽⁵⁵⁾. In addition, the HTSEL system should comply with other EU legislation such as the electromagnetic compatibility (EMC) Directive 2014/30/EU (EP and Council, 2014a) ⁽⁵⁶⁾, the Low-Voltage Directive (LVD) 2014/35/EU (EP and Council, 2014c) ⁽⁵⁷⁾, the general product safety Directive 2001/95/EC (EP and Council, 2001) ⁽⁵⁸⁾, the machinery Directive 2006/42/EC (EP and Council, 2006) ⁽⁵⁹⁾ and the Pressure Equipment Directive (PED) 2014/68/EU (EP and Council, 2014d) ⁽⁶⁰⁾. Test items which do not conform to these EU legislation shall not be used within the EEA.

⁽⁵¹⁾ WG 29 of TC 197 currently reviews this technical report.

⁽⁵²⁾ WG 34 of TC 197 currently prepares the AWI entitled "ISO 22734-1 Hydrogen generators using water electrolysis - Industrial, commercial, and residential applications — Part 1: General requirements, test protocols and safety requirements".

⁽⁵³⁾ In the future, IEC TC 105 may draft IEC 62282-8-200 on safety of power-to-power (P2P) systems using electrolyser complementing IEC 62282-8-201:2020 (IEC, 2020d).

⁽⁵⁴⁾ At present, this comprises the territories of the EU, Island, Norway and Liechtenstein. It also applies to Switzerland under a mutual recognition agreement and Türkiye under a customs union agreement with the EU.

⁽⁵⁵⁾ The EC publishes guidance online at https://single-market-economy.ec.europa.eu/single-market/european-standards/harmonised-standards/equipment-explosive-atmospheres-atex_en.

⁽⁵⁶⁾ The EC publishes guidance online at https://single-market-economy.ec.europa.eu/sectors/electrical-and-electronic-engineering-industries-eei/electromagnetic-compatibility-emc-directive_en.

⁽⁵⁷⁾ The EC publishes guidance online at https://single-market-economy.ec.europa.eu/sectors/electrical-and-electronic-engineering-industries-eei/low-voltage-directive-lvd_en.

⁽⁵⁸⁾ The EC publishes guidance online at https://single-market-economy.ec.europa.eu/single-market/european-standards/harmonised-standards/general-product-safety_en.

⁽⁵⁹⁾ The EC publishes guidance online at https://single-market-economy.ec.europa.eu/sectors/mechanical-engineering/machinery_en.

⁽⁶⁰⁾ The EC publishes guidance online at https://single-market-economy.ec.europa.eu/sectors/pressure-equipment-and-gas-appliances/pressure-equipment-sector/pressure-equipment-directive_en.

Annex B Tabulated data of operation profiles

B.1 Reactivity operation profile

Table B.1 contains the tabulated data of the reactivity operation profile (Figure 6.1).

Table B.1: Reactivity operation profile data.

Duration (s)	Normalised set point (%)
0	100
1	100
2	100
3	100
4	100
5	100
6	100
7	100
8	100
9	100
10	100
11	75
12	75
13	75
14	75
15	75
16	75
17	75
18	75
19	75
20	75
21	100
22	100
23	100
24	100
25	100
26	100
27	100
28	100
29	100
30	100
31	50
32	50
33	50
34	50
35	50
36	50
37	50
38	50
39	50
40	50
41	100
42	100
43	100
44	100
45	100
46	100
47	100
48	100
49	100

Continue to next page

Table B.1 – continued from previous page

50	100
51	25
52	25
53	25
54	25
55	25
56	25
57	25
58	25
59	25
60	25
61	100
62	100
63	100
64	100
65	100
66	100
67	100
68	100
69	100
70	100
71	0
72	0
73	0
74	0
75	0
76	0
77	0
78	0
79	0
80	0
81	100
82	100
83	100
84	100
85	100
86	100
87	100
88	100
89	100
90	100
91	25
92	25
93	25
94	25
95	25
96	25
97	25
98	25
99	25
100	25
101	100
102	100
103	100
104	100
105	100
106	100

Continue to next page

Table B.1 – continued from previous page

107	100
108	100
109	100
110	100
111	50
112	50
113	50
114	50
115	50
116	50
117	50
118	50
119	50
120	50
121	100
122	100
123	100
124	100
125	100
126	100
127	100
128	100
129	100
130	100
131	75
132	75
133	75
134	75
135	75
136	75
137	75
138	75
139	75
140	75
141	100
142	100
143	100
144	100
145	100
146	100
147	100
148	100
149	100
150	100
151	100
152	100
153	100
154	100
155	100
156	100
157	100
158	100
159	100
160	100

Source: JRC, 2020 (Tsotridis and Pilenga, 2021).

B.2 Flexibility operation profiles

Table B.2, Table B.3 and Table B.4 contain the tabulated data of the high flexibility operation profile (Figure 6.2), the 100 % flexibility operation profile (Figure 6.3) and the 200 % flexibility operation profile (Figure 6.4), respectively.

Table B.2: High flexibility operation profile data.

Duration (min)	Normalised set point (%)
1	25
2	25
3	25
4	25
5	25
6	25
7	25
8	25
9	25
10	25
11	25
12	25
13	25
14	25
15	25
16	50
17	50
18	50
19	50
20	50
21	50
22	50
23	50
25	50
26	50
27	50
28	50
29	50
30	50
31	75
32	75
33	75
34	75
35	75
37	75
38	75
39	75
40	75
41	75
42	75
43	75
44	75
45	75
46	100
47	100
48	100
49	100
50	100
51	100
52	100

Continue to next page

Table B.2 – continued from previous page

53	100
54	100
55	100
56	100
57	100
58	100
60	100
62	125
63	125
65	125
66	125
67	125
68	125
69	125
70	125
71	125
73	125
74	125
75	125
76	150
77	150
78	150
79	150
80	150
81	150
82	150
83	150
84	150
85	150
87	150
88	150
89	150
90	150
91	175
92	175
93	175
94	175
95	175
96	175
97	175
98	175
99	175
100	175
101	175
102	175
103	175
104	175
105	175
106	200
108	200
109	200
110	200
112	200
113	200
114	200
115	200
116	200

Continue to next page

Table B.2 – continued from previous page

117	200
118	200
119	200
120	200
121	100
122	100
123	100
124	100
125	100
126	100
127	100
128	100
129	100
130	100
131	100
132	100
133	100
134	100
135	100
136	50
137	50
138	50
139	50
140	50
141	50
142	50
143	50
144	50
145	50
146	50
147	50
148	50
149	25
151	25
153	25
155	25
156	25
157	25
158	25
159	25
160	25
161	25
162	25
163	25
164	25
165	25

Source: JRC, 2020 (Tsotridis and Pilenga, 2021).

Table B.3: 100 % flexibility operation profile data.

Duration (min)	Normalised set point (%)
1	25
2	25
3	25
4	25
5	25

Continue to next page

Table B.3 – continued from previous page

6	25
7	25
8	25
9	25
10	25
11	25
12	25
13	25
14	25
15	25
16	50
17	50
18	50
19	50
20	50
21	50
22	50
23	50
24	50
25	50
26	50
27	50
28	50
29	50
30	50
31	75
32	75
33	75
34	75
35	75
36	75
37	75
38	75
39	75
40	75
41	75
42	75
43	75
44	75
45	75
46	100
47	100
48	100
49	100
50	100
51	100
52	100
53	100
54	100
55	100
56	100
57	100
58	100
59	100
60	100
61	75
62	75

Continue to next page

Table B.3 – continued from previous page

63	75
64	75
65	75
66	75
67	75
68	75
69	75
70	75
71	75
72	75
73	75
74	75
75	75
76	50
77	50
78	50
79	50
80	50
81	50
82	50
83	50
84	50
85	50
86	50
87	50
88	50
89	25
90	25
91	25
92	25
93	25
94	25
95	25
96	25
97	25
98	25
99	25
100	25
101	25
102	25
103	25
104	25
105	25

Source: JRC, 2020 (Tsotridis and Pilenga, 2021).

Table B.4: 200 % flexibility operation profile data.

Duration (min)	Normalised set point (%)
1	25
2	25
3	25
4	25
5	25
6	25
7	25
8	25

Continue to next page

Table B.4 – continued from previous page

9	25
10	25
11	25
12	25
13	25
14	25
15	25
16	50
17	50
18	50
19	50
20	50
21	50
22	50
23	50
24	50
25	50
26	50
27	50
28	50
29	50
30	50
31	75
32	75
33	75
34	75
35	75
36	75
37	75
38	75
39	75
40	75
41	75
42	75
43	75
44	75
45	75
46	100
47	100
48	100
49	100
50	100
51	100
52	100
53	100
54	100
55	100
56	100
57	100
58	100
59	100
60	100
61	125
62	125
63	125
64	125
65	125

Continue to next page

Table B.4 – continued from previous page

66	125
67	125
68	125
69	125
70	125
71	125
72	125
73	125
74	125
75	125
76	150
77	150
78	150
79	150
80	150
81	150
82	150
83	150
84	150
85	150
86	150
87	150
88	150
89	150
90	150
91	175
92	175
93	175
94	175
95	175
96	175
97	175
98	175
99	175
100	175
101	175
102	175
103	175
104	175
105	175
106	200
107	200
108	200
109	200
110	200
111	200
112	200
113	200
114	200
115	200
116	200
117	200
118	200
119	200
120	200
121	175
122	175

Continue to next page

Table B.4 – continued from previous page

123	175
124	175
125	175
126	175
127	175
128	175
129	175
130	175
131	175
132	175
133	175
134	175
135	175
136	150
137	150
138	150
139	150
140	150
141	150
142	150
143	150
144	150
145	150
146	150
147	150
148	150
149	150
150	150
151	125
152	125
153	125
154	125
155	125
156	125
157	125
158	125
159	125
160	125
161	125
162	125
163	125
164	125
165	125
166	100
167	100
168	100
169	100
170	100
171	100
172	100
173	100
174	100
175	100
176	100
177	100
178	100
179	100

Continue to next page

Table B.4 – continued from previous page

180	100
181	75
182	75
183	75
184	75
185	75
186	75
187	75
188	75
189	75
190	75
191	75
192	75
193	75
194	75
195	75
196	50
197	50
198	50
199	50
200	50
201	50
202	50
203	50
204	50
205	50
206	50
207	50
208	50
209	25
210	25
211	25
212	25
213	25
214	25
215	25
216	25
217	25
218	25
219	25
220	25
221	25
222	25
223	25
224	25
225	25

Source: JRC, 2020 (Tsotridis and Pilenga, 2021).

Annex C Test report

C.1 General

The test report shall accurately, clearly and objectively present all relevant information to demonstrate whether or not the purpose(s) and objective(s) of the test is/are attained. As a minimum requirement, the test report shall contain a title page (section C.2) and a summary report (section C.3) with the measured or estimated TIPs and TOPs at least as mean values along with their (combined) standard uncertainties whether absolute, relative or both. The test plan (section 6.5) as executed may be appended to the report. Calibration records and/or certificates of the measuring instruments used may also be appended to the report.

C.2 Title page

The titlepage shall present the following information:

- (a) report identification, *i. e.* report number (optional),
- (b) type of report (summary, detailed or full),
- (c) author(s) of the report,
- (d) entity issuing the report with name and address,
- (e) date of the report,
- (f) person(s) conducting the test when different from the reporting author(s),
- (g) organisation conducting the test when different from report issuing entity,
- (h) date and time per test run,
- (i) location per test run when different from the address of the report issuing entity,
- (j) descriptive name per test and
- (k) identification (model name, serial number, type and specification) of the HTE stack and/or HTSEL system tested including their manufacturer(s).

The titlepage may be followed by a contents page before the summary report.

C.3 Summary report

The summary report shall include the following information:

- (i) test purpose(s) and objective(s),
- (ii) description of the test(s) with sufficient information on the test conduct and measurement set-up including test methods, measurement techniques (section 6.4) and test conditions (section 6.2),
- (iii) all relevant test parameters namely TIPs and TOPs including uncertainties (section 7) as well as
- (iv) conclusion(s) including graphical presentation of test results (section 7) and discussion with remark(s) and/or observation(s) as appropriate.

GETTING IN TOUCH WITH THE EU

In person

All over the European Union there are hundreds of Europe Direct centres. You can find the address of the centre nearest you online (european-union.europa.eu/contact-eu/meet-us_en).

On the phone or in writing

Europe Direct is a service that answers your questions about the European Union. You can contact this service:

- by freephone: 00 800 6 7 8 9 10 11 (certain operators may charge for these calls),
- at the following standard number: +32 22999696,
- via the following form: european-union.europa.eu/contact-eu/write-us_en.

FINDING INFORMATION ABOUT THE EU

Online

Information about the European Union in all the official languages of the EU is available on the Europa website (european-union.europa.eu).

EU publications

You can view or order EU publications at op.europa.eu/en/publications. Multiple copies of free publications can be obtained by contacting Europe Direct or your local documentation centre (european-union.europa.eu/contact-eu/meet-us_en).

EU law and related documents

For access to legal information from the EU, including all EU law since 1951 in all the official language versions, go to EUR-Lex (eur-lex.europa.eu).

Open data from the EU

The portal data.europa.eu provides access to open datasets from the EU institutions, bodies and agencies. These can be downloaded and reused for free, for both commercial and non-commercial purposes. The portal also provides access to a wealth of datasets from European countries.

The European Commission's science and knowledge service

Joint Research Centre

JRC Mission

As the science and knowledge service of the European Commission, the Joint Research Centre's mission is to support EU policies with independent evidence throughout the whole policy cycle.



EU Science Hub
joint-research-centre.ec.europa.eu



@EU_ScienceHub



EU Science Hub - Joint Research Centre



EU Science, Research and Innovation



EU Science Hub



EU Science



Publications Office
of the European Union